New Methods and Applications in Solid-State NMR Spectroscopy of Quadrupolar Nuclei

Sharon E. Ashbrook* and Scott Sneddon

School of Chemistry, EaStCHEM and Centre of Magnetic Resonance, University of St Andrews, St Andrews KY16 9ST, United Kingdom

*Email: *sema@st-andrews.ac.uk*

Invited Perspectives article for *J. Am Chem. Soc.*

Abstract

Solid-state nuclear magnetic resonance (NMR) spectroscopy has long been established as offering a unique atomic-scale and element-specific insight into the structure, disorder and dynamics of materials. NMR spectra of quadrupolar nuclei ($I > 1/2$) are often perceived as being challenging to acquire and to interpret, owing to the presence of anisotropic broadening arising from the interaction of the electric field gradient and the nuclear electric quadrupole moment, broadening the spectral lines, often over several MHz. Despite the vast amount of information contained in the spectral lineshapes, the problems with sensitivity and resolution have, until very recently, limited the application of NMR of quadrupolar nuclei in the solid state. In this Perspective, we provide a brief overview of the quadrupolar interaction, describe some of the basic experimental approaches used for acquiring high-resolution NMR spectra and discuss the information that these spectra can provide. We then describe some interesting recent examples to showcase some of the more exciting and challenging new applications of NMR spectra of quadrupolar nuclei in the fields of energy materials, microporous materials, Earth sciences and biomaterials. Finally, we consider the possible directions that this highly informative technique may take in the future.

1. Introduction

Among the most important aims of the solid-state chemist is the ability to predict and control the properties of compounds and, therefore, to design a material (and the requisite synthetic route) specifically for a particular application. Key to this is an understanding of the structure-property-function relationships in the solid state, with the first, and perhaps most vital, step being a detailed structural characterisation. Historically, this has been achieved using techniques based on Bragg diffraction, relying on the presence of the long-range order characteristic of many solids. While extremely powerful for ordered crystalline solids, diffraction typically produces a structural picture averaged over both time and lengthscale. As many of the interesting properties of solids (such as the activity of microporous catalysts, the radiation resistance and durability of ceramics or the capacity of energy materials) arise from the variation of this periodic nature, the use of spectroscopic techniques, which have the ability to probe the detailed atomic-scale structure, is a vital, and yet often overlooked, complementary approach. Nuclear magnetic resonance (NMR) spectroscopy has long been heralded as a sensitive probe of the local environment in solids, able to provide detailed information on structure and disorder in the solid state, while its sensitivity to motion over a wide range of timescales also enables dynamics to be investigated.[1,2] The use of ^{1}H, ^{13}C, ^{29}Si and ^{31}P NMR spectroscopy has had a significant impact in the pharmaceutical industry, materials chemistry, geochemistry and industrial chemistry, for the study of drugs and active pharmaceuticals, catalysts, glasses, zeolites and minerals.[3-10]

Unlike their solution-state counterparts, NMR spectra of solids are affected by anisotropic, or orientation-dependent interactions, including the chemical shift anisotropy (CSA) and the dipolar coupling, preventing the extraction of site-specific information.[1-2] These interactions are averaged by molecular tumbling in solution, providing spectra with higher sensitivity and high resolution. Approaches to remove anisotropic broadening in the solid state, such as magic-angle spinning (MAS)[11] and decoupling,[12] are available, and

for nuclei with spin quantum number I = 1/2, high-resolution or isotropic spectra can be obtained. The NMR spectra of quadrupolar nuclei, *i.e.*, those with I > 1/2, are additionally affected by an interaction with the electric field gradient at the nucleus.[13,14] The anisotropic quadrupolar broadening can be significant, with lineshapes broadened over many MHz. Furthermore, this anisotropy cannot be removed completely by MAS, and so spectra remained broadened even when the sample is rotated.[13,14] Although, in principle, the quadrupolar interaction provides an additional probe of the local structure and geometry, more usually, the anisotropic broadening prevents the resolution of distinct lineshapes, and makes the acquisition of detailed information significantly more challenging.

Over 74% of the nuclides in the Periodic Table have spin quantum number I > 1/2, and for over 63% elements the only NMR-active isotopes are quadrupolar, meaning that there are no I = 1/2 counterparts available for study. However, quadrupolar nuclei, such as ^{2}H, $^{6/7}$Li, ^{11}B, ^{14}N, ^{17}O, ^{23}Na, ^{25}Mg, ^{27}Al, ^{35}Cl, ^{39}K, ^{59}Co, $^{69/71}$Ga and ^{93}Nb, are of importance across the fields of chemistry, physics, biology, materials science and geology, as they are present in inorganic oxides, functional materials and ceramics, glasses and clays, polymers, pharmaceuticals and biomaterials, energy materials and in the compounds that make up the inner layers of our own planet.[1,2,14-20] The development of methods for studying these nuclei using NMR spectroscopy, and the ability to exploit the site-specific and atomic-scale structural information this provides is, therefore, crucial.

In this Perspective, after briefly reviewing the quadrupolar interaction, the experimental approaches used for acquiring NMR spectra of quadrupolar nuclei, and the methods used to achieve high resolution, we will consider how NMR spectroscopy of quadrupolar nuclei can provide information on structure, disorder, dynamics and reactivity in the solid state, highlighting some recent methodological and theoretical advances. We will also consider some examples of the more exciting and challenging applications of NMR spectroscopy to a range of different materials, including energy materials, biomaterials, geologically-relevant materials and functional solids. Finally, we

will conclude by considering where future advances will take this field and the challenges that will remain. By its very nature, a Perspective cannot be a comprehensive review of the area, and readers are also referred to Ref. 14 (and all articles within) for a more complete general overview and detailed discussion of specific areas.

2. Background and basic experiments

Solid-state NMR spectra of quadrupolar nuclei are dominated by the interaction between their nuclear electric quadrupole moment, eQ, and the electric field gradient (EFG) at the nucleus.[13] The EFG can be defined in its principal axis system by three components, V_{XX}, V_{YY} and V_{ZZ}, and is usually described in terms of its magnitude, given by the quadrupolar coupling constant, $C_Q = eQV_{ZZ}/h$, and an asymmetry (or shape), $\eta_Q = (V_{XX} - V_{YY})/V_{ZZ}$, such that $0 \leq \eta_Q \leq 1$. The quadrupolar interaction can be very large, with C_Q values of many hundreds of kHz to tens (and even hundreds) of MHz.[1,2,13] Despite this, in most practically-relevant cases the quadrupolar interaction remains smaller than the dominant Zeeman interaction, and its effect upon the nuclear spin energy levels is described using perturbation theory. Figure 1 shows the perturbation of the Zeeman energy levels caused by the quadrupolar interaction for nuclei with I = 1 and I = 3/2, and the lifting of the degeneracy of the single-quantum transitions. For the powdered solids most typically studied, different crystallite orientations result in a large anisotropic broadening, although for half-integer spins the central transition (CT) remains relatively sharp and is, in many cases, the only transition observed experimentally.[1,2,13]

The standard technique for improving resolution in solid-state NMR is MAS,[11] where the sample is rapidly rotated around an axis inclined at an angle of 54.736° to the external magnetic field, as shown in Figure 2a. Samples are packed into rotors of varying diameter (Figure 2b), with the maximum possible MAS rate increasing as the rotor diameter decreases. The smallest commercially-available rotors, with diameters of 0.75 mm, can be rotated at rates of over 100 kHz. For anisotropic interactions to be removed

efficiently, the rotation must be fast (relative to the magnitude of the interaction). This is usually achievable for the CSA and many dipolar couplings. However, the magnitude of the quadrupolar interaction is often such that complete averaging is not possible, and the lineshape is broken up into a series of spinning sidebands,[1,2,14] separated by integer multiples of the spinning rate, as shown by the ^{2}H (I = 1) NMR spectra of oxalic acid in Figure 2c,[21] where MAS resolves two resonances, corresponding to OD and D_2O species.

In many cases, the magnitude of the quadrupolar interaction is such that the first-order perturbation shown in Figure 1 is not sufficient to describe its effect upon the nuclear energy levels, and higher-order perturbations must be considered.[13] All transitions are affected by the second-order quadrupolar interaction, which has both an isotropic component (with the important result that the resonance position no longer reflects only the chemical shift), and anisotropic components (that lead to additional line broadening), as shown by the ^{71}Ga (I = 3/2) NMR spectra of $GaPO_4$ berlinite (a simple compound with a single Ga site) in Figure 2d.[22] The second-order broadening increases with C_Q, but decreases as the B_0 field strength increases, making the use of high magnetic fields particularly beneficial for quadrupolar nuclei. As the second-order quadrupolar interaction has a more complex angular dependence, it is only partially averaged under MAS and a powder-pattern lineshape is still obtained, as can be seen in Figure 2d for $GaPO_4$ berlinite.[22] Simple lineshape fitting enables the extraction of the NMR parameters. However, while this is straightforward when only one resonance is present, for materials containing a number of distinct species the lineshapes may overlap, as shown in Figure 3a for the ^{23}Na MAS spectrum of $Na_4P_2O_7$ (with four distinct Na species), and it is difficult to extract the relevant information from the complex lineshape.[23]

If the magnitude of the quadrupolar interaction is large (a problem exacerbated at low B_0 fields or for nuclei with low γ), even CT lineshapes may be broadened such that MAS is not able to improve resolution, as sufficiently fast rotation rates are not possible. In these cases, it is simplest to obtain a wideline spectrum on a static sample.[24] If the

lineshapes are very broad, spectra must be acquired in a piecewise manner, with a number of experiments performed at different transmitter frequencies and added together to produce the final spectrum. Recent work by Schurko and co-workers[24-28] has considerably eased the acquisition of wideline spectra, through the implementation of pulses (*e.g.*, WURST) that offer more broadband excitation, resulting in improvements in the spectra obtained, and reductions in the time taken to acquire them. For wideline experiments sensitivity is a particular challenge, and many approaches have been used to overcome this, including Carr–Purcell–Meiboom–Gill (CPMG) echo trains,[29] and manipulation of the population of the nuclear energy levels using FAM-type[30] pulses, double frequency sweeps[31] or shaped hyperbolic secant pulses.[14,32] Most approaches used are equally applicable to rotating samples, and can be used in conventional MAS experiments. See Refs. 33 and 34 for more detail in this area.

The combination of broadband pulses and sensitivity improvements, coupled with the recent availability of high magnetic fields, has certainly resulted in a step change in the quality of wideline spectra that can be obtained and expanded the range of materials able to be studied, with this approach recently applied to *e.g.*, ^{35}Cl of organometallic complexes,[35] ^{25}Mg NMR in minerals,[36] ^{87}Sr NMR of carboxylates,[37] ^{115}In complexes,[38] inorganic ^{135}Ba compounds,[39] ^{79}Br and ^{127}I NMR,[18] and the acquisition of ^{14}N (I = 1) spectra.[40] While interesting correlations of the NMR parameters with structural features such as the nature of ligand binding[35] or the strength of halogen bonds,[41] have been observed, applications do seem restricted to cases where the number of overlapped lineshapes is very small, and where other interactions (such as dipolar couplings) do not significantly affect the spectra. In many cases, removal of the broadening and resolution of distinct sites will be required before structural information can be obtained.

3. The quest for resolution

The broadening in the NMR spectra of quadrupolar nuclei limits both sensitivity and resolution and severely hampers the extraction of site-specific structural information. Perhaps the most enduring aim in solid-state NMR of quadrupolar nuclei over the last few decades, therefore, has been the complete removal of the quadrupolar broadening and the acquisition of high-resolution (isotropic) spectra and, although most major developments in this area are less recent, this subject has had such an impact on the history of NMR of quadrupolar nuclei, a brief review of the methods now used is warranted.

The orientational dependence of the second-order quadrupolar broadening is more complex than that of the CSA, dipolar couplings (or the first-order quadrupolar interaction), and cannot be removed by spinning around a single angle alone. The first approaches to solving this problem, developed in the late 1980s, were composite sample rotation techniques, *i.e.*, involving rotation of the sample around two different angles – simultaneously in the case of double rotation (DOR)[42] and sequentially for dynamic angle spinning (DAS).[43] Conceptually, DOR is easier to understand, with two rotors used, one inside the other. Each spins at a different angle (54.74° and 30.56°), to average the two different anisotropic components of the broadening. In DAS, the sample is sequentially rotated around two different angles (for different times) in a two-dimensional experiment,[42] with times and angles chosen such that the quadrupolar broadening is refocused. For further information on DOR and DAS see Ref. 14.

The study of quadrupolar nuclei in the solid state was revolutionised in 1995 by the introduction of the multiple-quantum (MQ) MAS experiment.[44] Unlike DAS and DOR, MQMAS uses sample rotation around a single angle (*i.e.*, 54.736°, thereby additionally removing CSA and dipolar interactions), and so can be performed using a conventional probehead. Removal of the second-order quadrupolar interaction is achieved within a two-dimensional experiment, where multiple-quantum (*e.g.*, $m_I = +3/2 \leftrightarrow m_I = -3/2$) coherences are correlated with CT coherences. The result is shown in Figure 3b, where the four distinct ^{23}Na species in $Na_4P_2O_7$ can now be resolved in the ^{23}Na MQMAS spectrum.[23]

Cross-sections enable the NMR parameters for each site to be determined individually, as shown in Figure 3c. For a more detailed discussion on MQMAS see Refs. 14, 45 and 46. A conceptually similar experiment, termed STMAS, using the correlation, not of multiple-quantum transitions but of the single-quantum satellite transitions (ST), was introduced in in 2000 by Gan,[47] as an alternative approach. Its implementation is more challenging than that of MQMAS (with the need for very accurate adjustment of the spinning angle (to ±0.002°), a stable spinning rate and accurate pulse timings), but it typically offers a significant sensitivity advantage over MQMAS (in many cases of factors between 4 and 8). For further information on STMAS see Refs. 14 and 48.

A pertinent question for the solid-state chemist is which of these established methods to choose? The literature shows that the most widely applied technique is MQMAS, which has enabled site resolution and extraction of structural information in many different chemical systems.[45-46] One obvious reason for this popularity is the need for only a conventional MAS probehead, whereas both DOR and DAS require dedicated hardware, and this has ensured they have remained largely within the realm of the specialist. The easy implementation of MQMAS is offset somewhat by its inherently poor sensitivity. Much effort has been focussed on improving this in recent years and good results have been obtained using the FAM, DFS and HS pulses discussed earlier, while the soft pulse added mixing (SPAM) approach provides sensitivity enhancement at relatively little additional cost.[6,30-32,49-50] Despite these advances, the poor efficiency of MQMAS can remain a problem for challenging samples and nuclei with inherently low sensitivity. Whilst STMAS also requires only conventional hardware (and has much greater sensitivity), the stricter requirements on its implementation appear to have restricted its use, with its greatest successes achieved when sensitivity is limited (*i.e.*, small sample volumes and nuclei with low natural abundance or low gyromagnetic ratio).[48] In recent years improved hardware has eased the implementation of STMAS and, although perhaps not fulfilling its true potential at present, it should become more popular in the future.

Recent hardware advances have, however, also seen a resurgence of interest in DOR, although the size of the outer rotor does still restrict the MAS rates that can be used, producing a range of spinning sidebands that can complicate spectral analysis. Impressive recent work has used DOR to investigate dipolar and J couplings between quadrupolar spins,[51-53] providing not only information on the fundamental nature, presence and magnitude of higher-order interactions[54] (of interest to the specialist), but important structural information of interest to the chemist. Figure 3d shows the ^{11}B DOR (top) and MAS (bottom) spectra of manganese catecholboryl pentacarbonyl. The coupling patterns revealed by DOR enabled information on the ^{55}Mn quadrupolar interaction to be extracted, enabling the observation that the interaction of Mn with the carbonyl ligands is stronger than that with catecholboryl ligand.[52]

The desire to remove the quadrupolar broadening and acquire high-resolution spectra has driven much research over the past few decades. However, with the progress made in recent years, it is now possible not only to achieve this almost routinely, but to combine experiments such as MQMAS and STMAS with the magnetisation transfer experiments commonly used in spin I = 1/2 NMR, enabling access to the full panoply of information NMR can provide.

4. Commonly-studied quadrupolar nuclei

The ease with which an NMR spectrum can be acquired is determined by a number of parameters including the natural abundance (N), spin quantum number (I) and gyromagnetic ratio (γ) of the nucleus. These are typically combined into a receptivity, given by $\gamma^3 N\ (I\ (I + 1))$, usually quoted relative to ^{1}H. However, for quadrupolar nuclei another important factor is the magnitude of the quadrupolar broadening of the spectral lines. Although for any specific material this depends upon the EFG and the Sternheimer antishielding factor,[55] the magnitude of the nuclear quadrupole moment is an important consideration. Table 1 gives the nuclear properties for some of the more commonly-

studied quadrupolar nuclei, and Figure 4 shows a plot of the receptivities, Larmor frequencies and quadrupole moments of a range of isotopes.[2,14]

Commonly-studied nuclei include those with reasonable natural abundance and small to medium quadrupolar coupling (*e.g.*, $^{6/7}$Li, ^{11}B, ^{23}Na, ^{27}Al, ^{45}Sc, *etc.*, as seen on Figure 4), while for nuclei with low natural abundance (such as ^{17}O) isotopic enrichment often has to be employed. For nuclei with low γ, such as ^{39}K and ^{25}Mg (see Figure 4), high magnetic field, and the sensitivity enhancement techniques discussed above, are usually required. Fast MAS is usually needed for nuclei exhibiting larger quadrupolar interactions, such as $^{69/71}$Ga and ^{93}Nb, while for species where the quadrupolar broadening is often much larger than available MAS rates (*e.g.*, $^{35/37}$Cl, $^{79/81}$Br, ^{127}I, ^{91}Zr, ^{87}Sr) the wideline approaches discussed above are preferred. Although NMR of nuclei with integer spin is typically quite different to that of nuclei with half-integer spin (owing to the lack of a narrow CT), and could indeed form the basis for an entire review or perspective in itself, it is worth mentioning the two most commonly-studied such nuclei here, ^{2}H and ^{14}N.[14, 56-57] Spectral acquisition is restricted to systems and species with smaller quadrupolar couplings (many ^{2}H species and ^{14}N in symmetrical environments) for MAS experiments, while wideline spectra of static samples are acquired for materials exhibiting larger C_Q.

5. Chemical structure and disorder

With diffraction firmly established as the method of choice among most chemists for the characterisation of solids, it is worth considering the information that NMR can provide and where its relative strengths lie. As nuclear spins are affected by a variety of structure-dependent interactions, NMR spectroscopy is able to provide detailed insight into the atomic-scale environment within a solid. On a basic level, the number of resonances and their relative intensities reveals the number and proportions of distinct species in the material, and so can confirm (or disprove!) the proposed symmetry or space

group. Although less straightforward than for I = 1/2 systems, this information can be obtained from many MAS spectra of quadrupolar nuclei, as shown in Figure 5a, where a ^{23}Na NMR spectrum of a novel vanadyl oxalatophosphate, $Na_2[(VO)_2(HPO_4)_2C_2O_4].2H_2O$ is able to distinguish between two proposed space groups, $P2_1/m$ and $P2_1$, obtained from refinements to the diffraction measurements.[58] The presence of two overlapping quadrupolar lineshapes, supports a space group of $P2_1$, rather than $P2_1/m$, where only a single distinct Na species would be expected. Spectroscopy can also identify minor impurities in materials (or those more difficult to distinguish by diffraction), that might have important effects upon the properties.[59-60] More generally, the magnitude of various NMR parameters can provide structural information, and many authors have attempted to determine (with varied success) the dependence of NMR parameters upon the local geometry for a range of quadrupolar nuclei.[2] The coordination number of a species can have a significant effect upon δ_{iso}, as illustrated by the ^{71}Ga (I = 3/2) spectra of the as-made and calcined GaPO-34 microporous frameworks shown in Figure 5b.[22] In the as-made sample, F^- anions bridge two Ga1 atoms, creating both four- (Ga2 and Ga3) and six-coordinate (Ga1) gallium. Upon calcination, a purely tetrahedral framework is produced, as shown by the change in chemical shift, while the symmetry change, from *P*–1 to *R*–3, is reflected in the presence of just one quadrupolar lineshape. Other well-known examples include the significant difference in ^{11}B C_Q values for trigonal (2-2.8 MHz) and tetrahedral (0-0.6 MHz) boron,[2] and the dependence of the ^{17}O C_Q upon the covalency of the X-O bond – an observation that allows bridging (*e.g.*, Si-O-Si) and non-bridging, (*e.g.*, Si-O-Mg), species to be distinguished in minerals and glasses.[19] Also commonly exploited in the study of biological and organic materials is the dependence of ^{2}H NMR parameters (both C_Q and δ_{iso}) on the geometry (*i.e.*, both distance and angle) of hydrogen bonds.[61]

Once a spectrum has been obtained the subsequent aim is to extract information on the type of species present (and how they might change with variation *e.g.*, in synthetic approach, in composition, over time or after reaction). Authors have previously sought to exploit the range of empirical relationships between NMR parameters and geometry, to

propose tentative spectral assignments.[2] However, considerable care must be taken as many different aspects of a structure can affect the NMR parameters. A classic example is the ^{27}Al NMR spectrum of andalusite (Al_2SiO_5), which contains two distinct Al sites, corresponding to five- and six-coordinate Al. Two resonances are observed in the spectrum, with C_Q values of 5.8 MHz and 15.3 MHz, respectively.[2,62] However, the latter results not from the five-coordinate Al as expected, but from the six-coordinate Al species, owing to a significant distortion of the coordination environment. In recent years, an alternative approach has been used to aid spectral understanding, exploiting the developments in the calculation of NMR parameters from first principles. Although used in conjunction with experiment in various areas of chemistry for many years, the need to approximate a solid as a cluster (centred on the atom of interest and with remote bonds terminated, typically by H), had limited the influence of computation in solid-state NMR spectroscopy. Interest in this area has been revitalised in recent years by the introduction of codes exploiting periodic boundary conditions to recreate the extended three-dimensional structure of a solid, most of which use density functional theory (DFT), a theoretical framework favoured for its cost-efficiency and accuracy.[63] The impact these methods have had on the experimental NMR community in particular has been significant, as evidenced by recent reviews.[64-66] Calculations play a key role in interpreting and assigning NMR spectra, as shown in Figure 5c, where quadrupolar-broadened ^{17}O NMR lineshapes (extracted from an STMAS spectrum) of the four distinct ^{17}O species in wadsleyite, β-Mg_2SiO_4, are compared to those predicted using DFT calculations.[8,67] Calculations not only enable assignment of the four oxygen species, but also verify the unexpectedly high experimental C_Q values[68] for the non-bridging species O3 and O4 (4.4 and 3.8 MHz, respectively), which are more typical of those expected for bridging oxygen atoms.

Although, in some cases, calculations are used to support and verify experimental measurements, their ultimate impact will result from the insight they provide for materials where the structure is not known or not fully defined, with the validity of

potential structural models able to be evaluated by comparing calculated and experimental NMR parameters. Calculations can also play a significant role in "NMR Crystallography",[69] where the combination of information from diffraction and NMR spectroscopy is used to provide quantitative structural detail, not able to be obtained from either method alone. The addition of computation (sometimes then referred to as "SMARTER Crystallography"), provides a link between the two experimental approaches. An excellent example of this is the recent work of Martineau *et al.*, where a structural model for a fluorinated inorganic-organic hybrid, $Zn_3Al_2F_{12}[HAmTAZ]_6$, (AmTAZ = 3-aminotriazole) was proposed using unit cell dimensions and a number of possible space groups (from diffraction), and the number and proportion of distinct species and their coordination environment (from ^{27}Al, ^{67}Zn, ^{19}F, ^{1}H, ^{15}N and ^{13}C NMR).[70] Possible models were then optimised, and ultimately validated, using DFT calculations. Although not yet perhaps routine, the combination of periodic calculations alongside experiment is now used frequently for simple systems, with the study of more complex materials beginning to be tackled with more advanced computational approaches. This has certainly been one of the most successful areas of recent development, and will undoubtedly have a wide and lasting impact on the field in the coming years.

Although information can be obtained from conventional NMR spectra, for detailed structural insight it is necessary to understand how the atoms in a structure are arranged in relation to each other. This can be achieved by probing the interactions between spins, either through space (for the dipolar interaction) or *via* covalent bonds (for the J coupling). Recently, there have been significant developments in the application of two-dimensional correlation experiments, previously used only for I = 1/2 nuclei, to quadrupolar spins. Both heteronuclear and homonuclear experiments are known, although the former are typically easier both to implement and to interpret,[14,20,71] and in many cases experiments are combined with MQMAS to improve resolution for the quadrupolar spin(s).[14,71,] The transfer of magnetisation through the heteronuclear J coupling is common, with, *e.g.*, $^{27}Al/^{31}P$, $^{71}Ga/^{31}P$ and $^{27}Al/^{17}O$ experiments all utilised.[71-75] However, the relatively small

J couplings for many quadrupolar nuclei have resulted in the greater development of approaches that exploit the (larger) dipolar interaction. A commonly-used approach for transferring magnetisation between spin I = 1/2 nuclei *via* the dipolar coupling is cross polarisation (CP). However, CP dynamics are significantly more complicated for quadrupolar nuclei,[76-77] with their efficiency dependent upon the radiofrequency (rf) field strength, the quadrupolar coupling and the spinning rate.[78-79] Alternative approaches utilised in recent years involve the use of trains of rf pulses to recouple (*i.e.*, reintroduce) the dipolar interaction in experiments initially designed to utilise J couplings.[6,71,80-84] Whilst a common complaint from the non specialist is that the vast number of possible experiments (and their often inexplicable acronyms) is confusing, essentially all experiments are similar – with the transfer of magnetisation from one type of spin to another, and a cross peak in the spectrum indicating the presence (and sometimes magnitude) of the interaction that they share. Advances, however, continue to be made, with one of the more recent being the introduction of a suite of methods for acquiring (indirectly) ^{14}N MAS spectra (see later for a more detailed discussion).[85-87] In general, this is an important area of considerable current development, and further progress over the next few years will ease both the choice (once the most efficient and more robust methods have been established) and implementation of these methods for a specific system for the general chemist.

For materials exhibiting a deviation from the periodicity associated with the solid state, *i.e.*, those with compositional or positional disorder, structure solution is considerably more challenging, and NMR provides a vital complementary tool to diffraction for the chemist. Disorder can give rise to many effects in the NMR spectrum, including additional or overlapped resonances and broadening of the spectral lines. For quadrupolar nuclei, distributions in both chemical shift and quadrupolar coupling constant can result, leading to additional broadening, and a characteristic "tail" to low frequency on the spectral lines. These lineshapes (and those in corresponding two-dimensional spectra) can be fitted to extract information on the distributions present using

a Czjzek model.[88] This broadening can make it more difficult to resolve overlapping contributions even when MQMAS is used, and information next nearest neighbour (NNN) atoms can be more difficult to obtain. This can be overcome to some extent by combining experiments with DFT calculations for a series of structural models where the local environment of an atom is varied and calculated NMR parameters can then be compared to experiment.[66,89-95] Some recent examples (see also later sections) include ^{27}Al NMR spectroscopy and DFT calculations to probe the Al/Si cation disorder in Gehlenite ($Ca_2Al_2SiO_7$),[91] where contributions from the seven Al local environments can be distinguished, and ^{27}Al/^{31}P NMR spectroscopy to investigate anion disorder in the AlPO framework STA-2.[92] For this latter case, as shown in Figure 6, the comparison of a range of ^{27}Al and ^{31}P NMR spectra, with the NMR parameters calculated for models with differing hydroxyl positions was able to show that hydroxyls bridge between Al1 and Al2 in the cancrinite cages, but that two hydroxyls do not occupy the same cage simultaneously.[90]

6. Dynamics and chemical reactivity

NMR spectroscopy has proven a useful probe of dynamics in the solid state, owing to its sensitivity to motion on timescales that vary over many orders of magnitude. This arises from a modulation of the resonance frequency caused by motion either of an atom itself, or of atom(s) in the local surroundings. Different motional timescales can be investigated, with fast motion (10^7 to 10^{11} s^{-1}) probed by changes in relaxation (not discussed in detail here), slow motions (10^3 to 10^{-1} s^{-1}) by exchange experiments, and rates intermediate to these extremes by changes to the spectral resonances. For quadrupolar nuclei, motion modulates the EFG tensor and so spectra are, therefore, sensitive to timescales determined by the inverse of the linewidth; typically 10^7 to 10^4 s^{-1} for resonances broadened by the first-order quadrupolar interaction and 10^5 to 10^3 s^{-1} for CT lineshapes subject to second-order quadrupolar broadening.[96]

One of the most commonly-exploited quadrupolar nuclei for studying dynamics is ^{2}H (I = 1), with typical linewidths (for static samples) of 1-200 kHz.[57,96-97] Furthermore, the ability to selectively deuterate provides site-specific motional information. The changes to the spectral lineshape as a function of temperature provide information on the geometry of the dynamic process and its rate, typically by comparison of experimental and simulated lineshapes.[97] Wideline experiments have also recently been demonstrated for ^{14}N in elegant work by Schurko and O'Dell, and offer similar potential for the future.[40,56,96] In addition to improving resolution and sensitivity, use of MAS is also able to extend the timescales that can be probed by ^{2}H NMR, with the width of the sidebands affected by the interference of motion with the averaging of the quadrupolar interaction by MAS.[21,96] In contrast to lineshape analysis, where the geometry of the motional process must be known, model-independent information (on the rate or activation energy) can be obtained from the linewidth variation with temperature, for each resolved resonance.[98-99]

For nuclei with half-integer spin quantum number, only the CT is typically observed. The shape and width of this second-order broadened lineshape is also sensitive to dynamics (at rates comparable to the magnitude of the interaction).[96] While comparison of experimental and simulated lineshapes will, in principle, be able to determine the type and rate of motion, the overlap of lineshapes in an MAS spectrum hinders the extraction of accurate and site-specific information. However, if resonances are reasonably well resolved, variable-temperature MAS experiments can provide information, and ^{17}O NMR in particular has been exploited in this manner by a number of authors.[96] An elegant example is the work of Hampson *et al*. who used two-dimensional ^{17}O exchange spectroscopy (EXSY) experiments to distinguish the motional model and timescale (10 s^{-1}) for the hopping of the WO_4 groups in ZrW_2O_8.[100] If multiple sites are overlapped in an MAS spectrum, high-resolution MQMAS or STMAS experiments may be used. As described above, MQMAS uses transitions not affected by the first-order quadrupolar interaction and so would only be affected by slower motion. In contrast, the STs are affected by the much larger first-order quadrupolar interaction, and motion on the

microsecond timescale results in a significant broadening of resonances. This was first demonstrated for a microporous phosphate framework, AlPO-14, where broadening of the ^{27}Al STMAS spectrum was observed as a result of motion of the template (isopropylammonium) within the pores of the material.[48,101]

The combination of DFT calculations and experiment can be particularly powerful when studying dynamics. One example of this is the recent investigation of clinohumite, $4Mg_2SiO_4.Mg(OH)_2$,[8,102-105] which exhibits two possible hydroxyl proton positions, H1 and H2 (see Figure 7a), each of which has a fractional occupancy (from diffraction) of 0.5. Figure 7b shows that the ^{17}O MQMAS spectrum, simulated by summing calculated spectra for different structural models, is in poor agreement with experiment. However, if the calculated ^{17}O NMR parameters are averaged prior to simulation, there is much better agreement, suggesting that there is dynamic, rather than static, disorder of the hydroxyl groups.[103] This is confirmed in Figure 7c, where the isotropic experimental ^{17}O STMAS spectra show significant broadening of some of the resonances, as a result of hydroxyl dynamics, and confirm $\log_{10}k = 5.5$.[101] The temperature-dependent MAS linewidth enables an activation energy of 40 ± 4 kJ mol^{-1} for H1/H2 exchange to be determined (Figures 7d and 7e).[104]

The sensitivity of NMR spectroscopy to local structure and to dynamics makes it a convenient tool for following physical and chemical transformations. These can be as simple as (de)hydration, apparent often from the change in coordination number of nuclei such as ^{27}Al and ^{71}Ga or, alternatively, more major changes to the NMR spectrum, as observed for some metal-organic framework (MOF) materials.[3,5,9] NMR can also be used to follow phase transitions as a function of temperature, or to probe the host-guest interactions in materials where small molecules can be chemisorbed or physisorbed. Chemical reactions can also be followed using NMR, with the nature of the products and reaction rate able to be probed. Transformations can be followed *ex situ*, *i.e.*, carrying out reactions under laboratory conditions, quenching at a variety of times and analysing the

products. Of considerably more use, however, is *in situ* study, which has the added advantage of enabling the detection of transient species. Simple (de)hydration processes can be easily followed, and in some cases occur inadvertently, owing to the frictional heating resulting from either MAS or decoupling. Such a reversible phase transition was observed for AlPO-53(A),[106] which dehydrated in the rotor to produce the related phase JDF-2 – a change that was immediately apparent from the ^{27}Al MAS NMR spectra. For more complex reactions *in situ* NMR can be challenging, both from a practical point of view (with the need to reproduce conditions, *i.e.*, temperature, pressure, reactant flow of a reaction, when the sample is spinning) and, for quadrupolar nuclei, from a spectroscopic point of view, with the presence of the quadrupolar broadening. For more ambitious reactions, *in situ* experiments are more usually performed on static samples, with hardware specially adapted to enable the reaction conditions to be as closely reproduced as possible (see below for examples). Although an exciting area (particularly for those interested in catalysis and small molecule storage) these experiments remain practically challenging and considerable advances are required before they can be considered in any sense routine. They do, however, perhaps offer one of the more interesting avenues for future development, as dynamics and reactions are often difficult to study in real time using other techniques.

7. Recent applications of solid-state NMR of quadrupolar nuclei

Solid-state NMR spectroscopy of quadrupolar nuclei has been widely applied to a range of problems in areas as diverse as chemistry, biology, geology and materials science. While a complete review is, of course, not practical in the context of a Perspective, below we highlight some recent applications in a few areas of current interest, to show what is presently possible. The reader is referred to the literature for more detailed reviews.[3,8-10,14-20]

Quadrupolar NMR of energy materials

Among the major challenges facing the world today are the growing threats from global warming, geopolitics and the finite amount of extractable fossil fuel reserves. It is anticipated that the world's energy systems will have to undergo a radical change in the near future, resulting in a pressing search for new energy materials that are efficient, clean and cost effective, both to produce and to operate. Solid-state NMR spectroscopy is ideally suited not only to the study of the local structure of such materials, but also the investigation of the dynamic and electrochemical processes that occur.[14,107-109] Research to date has focussed primarily on lithium battery materials and oxide ion conductors, with $^{6/7}$Li and ^{17}O NMR attracting considerable recent attention.[14,107-109] However, the experimental challenges posed here do not necessarily result from the quadrupolar nature of these nuclides, but from the need to understand the processes and structural changes that occur under operating conditions, *i.e.*, *in situ*, to be of real relevance.

Many investigations of energy materials exploit $^{6/7}$Li NMR spectroscopy, owing to the widespread use of lithium ion battery technology. Spectral acquisition is eased by small quadrupolar couplings and high sensitivity and, although diamagnetic materials exhibit a very small chemical shift range (typically a few ppm), the chemical shifts for Li in paramagnetic systems can be quite significant, often in the range of 1600 ppm.[2,107-109] Despite the success of Li ion batteries, the toxicity and cost of the most commonly-used cathode material, $LiCoO_2$, has prompted researchers to find viable alternatives. One promising series of materials are the layered lithium cobalt nickel manganese oxides, *i.e.*, $LiMO_2$ (where M = Ni, Mn, Co). Using ^{6}Li MAS NMR, Yoon *et al.*[110] were able to demonstrate that lithium was found both in the transition metal and lithium layers (the former demonstrated by the significant shifts resulting from the Ni^{2+} and Mn^{4+} neighbours), and both types of lithium were removed on charging. Similar structural investigations of a number of possible candidate materials have been undertaken using $^{6/7}$Li NMR, utilising the ability of the technique to probe local structure and its sensitivity to paramagnetic interactions.[14,107-109]

Of increasing interest, however, is the use of *in situ* NMR to investigate the production of transient states and the dynamic and chemical processes taking place in real time, during the operation of electrochemical devices.[107] In general, *in situ* experiments are performed (without the use of MAS) on entire devices connected to a potentiostat and NMR spectra are recorded as a function of the charge or discharge state, in approaches pioneered by Tarascon[111] and, more recently, by Grey.[107,112-113] In a recent example[113] *in situ* ^{11}B NMR was used for real-time studies of capacitors, investigating the adsorption of BF_4^- anions on highly porous carbon. Figure 8a shows the experimental setup used, modified from a flexible plastic bag cell design, separating the two electrodes so that only one is placed in the NMR coil.[113] This enables signals from the cathode or anode to be detected separately. Three resonances are observed in the NMR spectrum (see Figure 8b), corresponding to BF_4^- anions strongly bound in the double layers near the carbon electrode, weakly-bound ions (at downfield shifts), and a narrow peak resulting from free electrolyte. When the cell is charged the peaks from strongly- and weakly-bound BF_4^- begin to merge, while at more negative voltages the peak attributed to the strongly-bound anions is lost completely. Integration of the ^{11}B NMR resonances (Figure 8c) reveals a gradual decrease in the total signal intensity as the voltage decreases, consistent with the diffusion of BF_4^- ions to the electrode outside of the NMR coil. Similar experiments have been carried out for batteries, supercapacitors and fuel cells.[107-109]

In addition to battery and capacitor materials, the increasing application of oxide ion conductors in solid oxide fuel cells, sensors and separators has resulted in considerable NMR investigation of these materials.[109] Despite the need to isotopically enrich in many cases, ^{17}O NMR spectroscopy has emerged as the method of choice to investigate the local structure and the dynamic processes that take place. An elegant example of this type of study is the work of Kim and Stebbins, where ^{17}O NMR was used to study motion in Y-doped CeO_2, a promising solid-oxide electrolyte material.[114] A number of ^{17}O resonances were resolved and able to be assigned to environments with differing numbers of Y NNN.

Variable-temperature measurements showed coalescence between some of the peaks, with exchange between sites with Y neighbours occurring at a lower temperature than exchange involving sites distant from the dopant cation. Rapid exchange of all oxygen sites was observed above 400 °C. Such study will be vital in understanding and designing materials for future application.

Quadrupolar NMR of microporous materials

Microporous materials have found applications in gas storage and separation, catalysis and drug delivery, as their structures contain pores and channels of similar size to small molecules. Common microporous frameworks include (alumino)silicate zeolites, phosphate-based frameworks (also typically containing Al, Ga, Si, Mg, *etc.*, cations) and MOFs (with metal cations connected by organic linker molecules).[115] The basic constituents of these frameworks all contain NMR-active nuclei (many of which are quadrupolar), and in addition, mineralisers and structure directing agents (SDAs) also contain many nuclei suitable for study. For more detailed discussion see also Refs. 3, 5, 9, 14, and 116.

While the framework topology of microporous materials can often be determined using diffraction, NMR can provide additional detailed and element-specific information on framework substitution, the nature, disorder and dynamics of guests within the pores, and the position or disorder of charge-balancing species. NMR crystallographic approaches have found particular application in this area,[116-117] as evidenced by recent work on STA-2 (Figure 6), AlPO cloverite and AlPO-CJ2.[92,118-119] In the latter case, a variety of multinuclear NMR experiments were required in order to quantify the number and type of Al/P environments, and understand the framework structure and connectivity. However, using two-dimensional correlation experiments, such as the ^{19}F-^{27}Al J-HMQC spectrum shown in Figure 9a,[119] information about the OH^-/F^- distribution (not easily available from diffraction) was obtained. This spectrum shows that the bridging F^- species

(–115 ppm) is connected to both five- and six-fold Al species, while the terminal F^- (–125 ppm) is linked only to six-fold Al. The F^- species (–121 and –118 ppm), are linked to five-fold Al coordinated by OH. In other work, Beitone *et al*. used a combination of X-ray diffraction and NMR spectroscopy to distinguish between two proposed space groups, *I*–43*m* and *P*–43*n*, for a new zinc-aluminum phosphate $Zn_3Al_6(PO_4)_{12}.4tren.17H_2O$ (MIL-74).[120] More recently, Massiot *et al.* used a range of experiments (including three-dimensional $^{27}Al/^{31}P$ NMR experiments) to demonstrate that the unit cell of AlPO-40 contained 32 Al and 32 P sites, and was at least four times the size proposed initially.[121] The excellent resolution achieved (using decoupling) in ^{31}P MAS and ^{27}Al MQMAS spectra is shown in Figure 9b.

The great utility of microporous materials is their ability to selectively absorb and interact with guest molecules, either through interaction with framework metals or by adsorption into pores. As oxygen lines the pores of many microporous materials, it might seem that ^{17}O NMR spectroscopy should be a popular choice. However, application is limited by the low natural abundance of this isotope (0.037%). Many zeolites have been isotopically enriched using post-synthetic exchange with $^{17}O_2$ gas, and although extremely useful, care must be taken when interpreting peak intensities, unless the kinetics (and uniformity) of the exchange process are understood.[14,19] For aluminosilicates, resolution of ^{17}O NMR spectra can be limited unless the Si/Al ratio is high, but for materials with little cation disorder oxygen species can be resolved using MQMAS or DOR. As shown by the impressive work on the zeolite ferrierite, where 10 oxygen species are distinguished, variable field measurements are often vital.[122] Enrichment of phosphate frameworks is considerably more challenging as the SDA, and the framework itself, can break down at the temperatures used for gas exchange. Although solvothermal synthesis using $H_2{}^{17}O$ (l) is possible, this is costly and cost inefficient, with relatively little of the enriched material ending up in the framework. It has recently been shown, however, that cost-efficient ^{17}O enrichment is possible using ionothermal synthesis, where an ionic liquid is used as a solvent and only a small amount (10-20 μl) of $H_2{}^{17}O$ (l) is added.[123] Cost-effective ^{17}O

enrichment of MOFs (including MIL-53(Al) and CPO-27-Mg) has also been recently demonstrated by He *et al.*, with the reactants mixed and sealed in an autoclave that contained a small amount of $H_2{}^{17}O$ (l).[124] This work was also able to distinguish between bridging oxide and hydroxide ligands in UiO-66 - a task that would be almost impossible to achieve by diffraction techniques.[124]

MOFs exhibit a greater structural variation than zeolites or phosphate-based frameworks owing to the larger number of possible combinations of organic linkers and metals. Furthermore, with the growing possibility of post-synthetic modifications, an even greater variation of the structure is possible.[115] The study of MOFs using NMR spectroscopy has generally been limited to ^{1}H and ^{13}C (I = 1/2) experiments, although there have been some recent investigations of the metals.[9,116] For example, ^{27}Al and ^{45}Sc NMR have been used to study the motion and flexibility in MIL-53, where it is known that the MOF exhibits a so-called breathing motion, increasing the unit cell volume (by up to 230%) when a guest molecule is adsorbed.[125-126] In addition, ^{2}H NMR has been recently used to study the dynamics of the linker molecules in a number of MOFs, revealing that motions such as C_2 rotation of the benzene rings in terephthalate-based MOFs.[127-128]

Quadrupolar NMR in the Earth sciences

Solid-state NMR spectroscopy has had a significant impact in the field of geochemistry, with ^{29}Si (I = 1/2) NMR used extensively to study minerals, glasses and clays. However, the main constituents of our planet - crustal aluminosilicates and the deep Earth magnesium silicates, also contain quadrupolar nuclei, primarily ^{17}O, ^{27}Al and ^{25}Mg.[8,10,14] Natural minerals are complex multicomponent systems, which display considerable disorder – be it in the variation of cation/anion site occupancies, or in the detailed local structure and bonding. X-ray diffraction provides information on the average structure, and it falls to spectroscopy to probe local environment and dynamic processes in more detail. As shown in Table 1, ^{27}Al offers perhaps the best prospects for

straightforward study – with 100% natural abundance and high γ. For ^{17}O, isotopic enrichment is often required, while the relatively low natural abundance, low γ and large quadrupolar broadening combine to make ^{25}Mg NMR spectroscopy more of a challenge.

Many minerals and clays have been studied using ^{27}Al NMR spectroscopy,[8,10,14] although quadrupolar broadening prevents the resolution of distinct species unless MQMAS is used. The NMR parameters can often be related to local structural features, such as the distortion of coordination polyhedra or variation in cation-oxygen bond distances.[2,8,10] The dependence of the ^{27}Al chemical shift on coordination number has been exploited to help determined substitution mechanisms in natural minerals.[2,8,10] It is difficult to determine the effect of NNN substitutions, *e.g.*, cation site disorder, in aluminosilicates, owing to the quadrupolar broadening. More recently, however, the combination of experiment and calculation has offered an improved approach. This was elegantly demonstrated in the recent work of Massiot and co-workers, who investigated Al/Si ordering in gehlenite, $Ca_2Al_2SiO_7$.[91] Using MAS, MQMAS and two-dimensional $^{29}Si/^{27}Al$ HMQC experiments, seven distinct Al sites, Al-$(OAl)_{4-p}(OSi)_p$ and Al-$(OAl)_{3-p}(OSi)_p$ were identified. Comparison to DFT calculations of model structures determined that a purely random distribution of Al and Si (*i.e.*, not respecting Lowenstein's rule[129]) was present. This work really shows what is possible when state-of-the-art experiments and calculations are combined, and reflects the future direction of NMR crystallography.

Dynamic processes are of considerable interest in the Earth sciences, and many examples of investigations that use quadrupolar NMR spectroscopy (*e.g.*, ^{2}H, ^{17}O, ^{27}Al and ^{25}Mg) are known.[8,10,14] Of particular interest is the differentiation between static and dynamic disorder as, for example, in the case of the humite minerals shown in Figure 7, and described in detail above. In general, an understanding of OH^-/F^- disorder is a challenge in natural minerals, and is particularly difficult to probe using diffraction. Exchange between different sites in minerals can be probed using variable-temperature experiments, with notable examples including exchange of six- and eight-coordinate Na

environments in $Na_{0.95}K_{0.05}AlSiO_4$ (nepheline) using ^{23}Na NMR[14,130] and exchange of the two Mg sites in forsterite, α-Mg_2SiO_4, using ^{25}Mg NMR.[14,131]

The study of the deep Earth silicate minerals is hampered by the requirement to synthesise these materials at high pressure (*e.g.*, up to 130 GPa).[8,132] Use of a piston cylinder or a multi-anvil apparatus can restrict the amount of material available, to just a few mg in the latter case, limiting sensitivity and increasing the technical challenge of the measurements. Nonetheless, the recent advances in probe technology and greater availability of high magnetic fields have facilitated the study of such systems. Over the last few decades it has been recognised that the nominally-anhydrous minerals in the mantle can store significant quantities of hydrogen, typically referred to as water, at defects in the crystal lattice.[8] The advantages of using NMR to study these materials were highlighted in recent work combining experiment and DFT calculations to investigate the hydration of wadsleyite, β-Mg_2SiO_4.[133] Significant differences are seen in the STMAS (20.0 T) spectra of anhydrous and hydrous wadsleyite, as shown in Figures 10a and 10b, with a decrease in the intensity of O1 and an increase in a broad resonance attributed to OH^-. DFT calculations showed that the substitution was compensated by a Mg3 vacancy, and that the ^1H spectrum could only be matched by protonation not just of O1, but also of the O3/O4 silicate oxygens. This was confirmed by $^1H/^{17}O$ correlation experiments, as shown in Figure 10c, where Si-OH and Mg-OH species can be identified.[133]

Silicate glasses are of considerable importance at the Earth's surface, and their study can provide information on the composition of volcanic eruptions, heat and mass transfer within the Earth and the effects of weathering at the surface.[10,14] Such glasses are also of interest in materials science and technology, and in the remediation of nuclear waste. The lack of long-range order in glasses has provoked considerable interest in their study using NMR spectroscopy, an area that could form the topic of a complete review in itself.[134] Generally, the composition, speciation and cation disorder can be probed, although the variation in local geometry results in a distribution of NMR parameters and

while chemically-distinct species can be identified, resolution of individual sites is not possible.[134] In the context of the Earth Sciences, ^{27}Al and ^{17}O NMR spectroscopy are perhaps the most useful approaches, with ^{27}Al NMR spectra providing information on the Al coordination number, while ^{17}O MQMAS experiments are able to resolve Si-O-Si, Si-O-Al and Al-O-Al species, thus probing the extent of framework disorder.[135-137] Experiments on samples that have been rapidly quenched from high temperature, or experiments carried out under higher pressures, can be used to quantify the structural changes observed in glasses, with the most notable changes being increased coordination of Al (and Si) species with increasing pressure.[10,14,134]

Quadrupolar NMR of organic and biological materials

As one might expect, the most commonly-studied nuclei in NMR studies of organic and biological materials are ^{1}H, ^{13}C and ^{15}N.[2,6,7] As all have I = 1/2, high-resolution spectra are relatively easy to acquire (if fast MAS rates or high-power decoupling are available) and sensitivity can be enhanced by using CP. However, quadrupolar nuclei, such as ^{23}Na, ^{25}Mg, ^{39}K, ^{43}Ca, ^{63}Cu and ^{67}Zn, are abundant in biological systems, including proteins, enzymes and cell nuclei,[14,138,139] while nuclei such as ^{23}Na, ^{7}Li and ^{133}Cs have pharmacological application. In addition to the challenges faced for inorganic solids, there are often relatively few metal sites in biological systems, and many of the relevant species have low receptivities and/or significant quadrupolar broadening. This emerging area, therefore, had been facilitated more than most by the use of higher magnetic fields, advances in hardware and the introduction of sensitivity enhancement schemes.[14,33]

It has been estimated that at least one third of all proteins and enzymes that have been purified require metals for their biological function.[14] One such example is zinc-containing proteins, where the metal centre plays an important role in structure and catalysis. There are relatively few solid-state ^{67}Zn NMR studies, owing its low natural abundance (4.1%), low receptivity and large quadrupole moment (as shown in Figure 4).

Despite these challenges, in impressive work Lipton *et al.* were able to obtain ^{67}Zn CPMG NMR spectra for the wild type (WT) and the H265A mutant of *Aquifex aeolicus* LpxC.[140] A difference was observed in the ^{67}Zn spectrum with pH, as shown in Figure 11 for the WT protein. The appearance of a third Zn species at high pH (with a C_Q of 14.3 MHz) was attributed to changes in the protonation state of a nearby histidine residue, by comparison of the experimental measurements to theoretical calculations, providing insight into the structure of the protein at physiological conditions.

As with protein study, investigation of biomaterials using NMR spectroscopy has also primarily exploited spin I = 1/2 nuclei such as ^{13}C, ^{15}N and ^{31}P, owing to the ease of spectral acquisition. However, of considerable potential is ^{43}Ca (I = 7/2) NMR spectroscopy, as calcium can be found in naturally-occurring bone, tooth enamel and dentin.[141] Calcium can be challenging to study, owing to its very low natural abundance (0.135%) and the high cost of isotopic enrichment. A number of ^{43}Ca NMR investigations of bone and bone-related minerals have been performed,[141] with the first spectra of natural biominerals, a horse bone and a cow tooth, appearing in 2010.[142] In this work, a combination of ^{43}Ca solid-state NMR and Ca K-edge X-ray absorption spectroscopy provided information about the calcium coordination shell, and demonstrated a correlation of the ^{43}Ca chemical shift with the (average) Ca-O bond distance.[142] The complex nature of bone (a composite material where hydroxyapatite-like phases and an organic matrix are combined) has also led to considerable study of model apatite systems. In addition to the study of pure hydroxyapatite ($Ca_{10}(PO_4)_6(OH)_2$), which contains two distinct Ca sites, investigations have also focussed on possible substitutions of CO_3^{2-}, HPO_4^{2-}, Na^+ and Mg^{2+} into the apatite lattice.[142] The importance of biomaterials in the modern world will ensure this is an area of active research, with great benefit being obtained from higher magnetic fields.

Nitrogen is a key component of many biological, organic and pharmacological materials. The most abundant isotope (natural abundance 99.6%), ^{14}N, is quadrupolar (I =

1), although earlier study focussed on ^{15}N (I = 1/2) despite its low natural abundance (0.36%). As described above, ^{14}N does not exhibit a central transition and observation of all species (except those with symmetrical environments) was prohibitively time consuming until recent years. An increase in the availability of high-field measurements (and concomitant increases in sensitivity) brought some progress for wideline measurements, but perhaps the most significant advance in recent years has been the use of indirect detection experiments.[14,85-87] These MAS-based methods exploit the transfer of magnetisation between a spin I = 1/2 nucleus, typically ^{1}H or ^{13}C, and ^{14}N, with the ^{14}N MAS spectrum (exhibiting lineshapes broadened by the second- and sometimes third-order quadrupolar interaction). These have been used to provide information on ^{14}N quadrupolar couplings, C-N internuclear distances and dynamics in amino acids, small peptides and pharmaceutical compounds,[14,85-87] and represent an exciting area for future application.

8. Challenges and outlook

Since the first discussion of quadrupolar interactions in 1950[143] paved the way for the study of nuclei with spin I > 1/2 by NMR spectroscopy, the impressive developments in sophisticated hardware and the complex, yet elegant, pulse sequences introduced have enabled a wide application across the scientific disciplines. Despite often being viewed as the poor relation of I = 1/2 NMR spectroscopy, the study of quadrupolar nuclei, although admittedly technically more challenging, has the potential to offer more information (as a result of the additional interactions the nuclear spins experience) and is applicable to a greater proportion of the Periodic Table. An ongoing challenge is unquestionably the acquisition of high-resolution spectra (or alternatively the separation of the components of a composite spectral lineshape) in a cost-efficient and rapid manner. The presence of second-order quadrupolar broadening limits the utility of MAS, but we can surely look forward in the future to advances in technology and hardware that will significantly ease the practical implementation (and thus improve the performance) of experiments such as

DOR[42] and STMAS.[48] It is indisputable that NMR study of quadrupolar nuclei was revolutionised by the introduction of MQMAS,[44] and this has enabled a far greater applicability than was envisaged in the early 1990s. However, difficulties still remain with this method, with the need for improved sensitivity, both in absolute terms and per unit time. Possible solutions could be the use of more complex pulses, or changes to the way spectra are acquired. It has been demonstrated that some multidimensional spectra can be obtained in a single scan or step[144] and, while this is currently difficult to implement in every experiment, future software advances may make this routine for many spectra in the near future.

Although the faster MAS rates currently available contribute to improved spectral resolution, the limited sample volumes compound the second significant challenge that afflicts NMR spectroscopy of quadrupolar nuclei – that of sensitivity. The increasing availability of high-field measurements will certainly help this problem, and the recent developments in microcoil technology (enabling extremely strong rf fields to be achieved) should mitigate, at least to some extent, the limiting sensitivity of small volumes.[145] This will also enable better decoupling to be used, and simultaneously, therefore, aid resolution. It may be that additional advances will also be forthcoming if increased effort could be expended on the development of better methods for isotopic enrichment, with modifications to existing synthetic procedures able to significantly reduce the cost (in terms of both time and money). However, perhaps the technique generating the most interest in this regard is that of dynamic nuclear polarisation (DNP),[146] in which the transfer of polarisation from unpaired electrons to nuclei is able to provide significant signal enhancements. Although to date, largely applied to organic solids, porous materials and surfaces, exploiting both rapid spin diffusion among ^{1}H spins (prior to transfer to the nuclear species of interest) and easier introduction of the polarising agent, more recent work has been focussed on quadrupolar nuclei and inorganic solids.[147-149] Given the need for the development of reliable protocols for sample preparation, and an improved understanding of the experiment-, sample- and distance-dependent enhancements

observed, only time will tell if DNP will prove to be the panacea that is suggested, but it is certainly an exciting area requiring future research investment.

One clear future direction for improving the understanding of solid-state structure is the need for a closer relationship between the complementary diffraction-based and spectroscopic methods. This will enable a detailed picture of a material on a range of lengthscales and timescales to be constructed – essential if its physical and chemical properties are to be understood and, therefore, exploited. Computation may well be the key here – easing not only the understanding, interpretation and assignment of the complex spectral lineshapes observed, but enabling the prediction of NMR parameters for potential structural models and subsequent comparison to NMR experimental measurements. The greatest impact might well arise from the widening interest in methods for the generation of possible structural models prior to the calculation of NMR parameters, both in terms of high-throughput calculations in disordered systems and from first-principles (as in the *ab initio* random structure searching or AIRSS[150] approach).

An important goal for NMR spectroscopy is the understanding of the structural changes that occur during phase transitions, adsorption and chemical reactions. While progress has been made in many areas using *ex situ* measurements, *i.e.*, following an external reaction or process by quenching at various stages and subsequently analysing the material produced, the ultimate aim would be to follow these process *in situ*, with the procedure carried out inside the spectrometer directly. Variable-temperature experiments are possible (although measurements at more extreme conditions remain technically challenging and often the realm of specialists). Measurements have been made *in situ* and *operando*,[107,151-152] but the need to consider problems including flow of reactants and removal of products in a reaction, changes in electrochemical properties, density or volume of a solid during a phase transition, or the generation of gases in a reaction, make the combination of these experiments with sample rotation extremely challenging. However, the potential impact of such measurements does make this an essential direction

for future research.

It is clear that much more technological and methodological development is required before NMR spectroscopy of quadrupolar nuclei can achieve anywhere near its full potential. However, the consistent progress made over the last few decades augurs well for further advances in the years to come. It is to be hoped that researchers of the future will view NMR spectroscopy as an important component of a suite of analytical techniques that should be combined to provide detailed information on structure, disorder and dynamics in the solid state.

Acknowledgements

The authors acknowledge EPSRC for the award of a studentship to SS. The authors also thank Dr Daniel Dawson and Dr Valerie Seymour for their help in the preparation of this manuscript.

References

1. Apperley, D. C.; Harris, R. K.; Hodgkinson, P. *Solid State NMR Basic Principles and Practice*, Momentum Press, New York, 2012.

2. MacKenzie, K. J. D.; Smith, M. E. *Multinuclear Solid-State NMR of Inorganic Materials*, Pergamon Press, Oxford, 2002.

3. Klinowski, J. *Prog. Nucl. Magn. Reson. Spectrosc*. **1984**, *16*, 237-309.

4. Eckert, H. *Prog. Nucl. Magn. Reson. Spectrosc*. **1992**, *24*, 159-293.

5. Klinowski, *J. Anal. Chim. Acta*. **1993**, *283*, 929-965.

6. Brown, S. P. *Macromol. Rapid Commun.* **2009**, *30,* 688-716.

7. Hodgkinson, P. *Ann. Rep. NMR Spectrosc.* **2010**, *72*, 185-223.

8. Ashbrook, S. E.; Griffin, J. M. *Ann. Rep. NMR Spectrosc*. **2013**, *79*, 241-332.

9. Sutrisno, A.; Huang, Y. *Solid State Nucl. Magn. Reson*. **2013**, *49-50*, 1-11.

10. Stebbins, J. F.; Xue, X. Y. *Spectroscopic Methods in Mineralogy and Materials Sciences*, Mineralogical Society of America, Chantilly, 2014.

11. Andrew, E. R.; Bradbury, A.; Eades, R. G. *Nature* **1958**, *182*, 1659-1659.

12. Hodgkinson, P. *Prog. Nucl. Magn. Reson. Spectrosc.* **2005**, *46*, 197-222.

13. Vega, A. J. *Quadrupolar Nuclei in Solids*, eMagRes, 2010. DOI: 10.1002/9780470034590.emrstm0431.pub2.

14. Wasylishen, R. E.; Ashbrook, S. E.; Wimperis, S. (Eds) *NMR of Quadrupolar Nuclei in Solid Materials*, John Wiley & Sons Ltd, Chichester, 2012.

15. Fernandez, C.; Pruski, M. *Topics in Curr. Chem*. **2012**, *306*, 119-188.

16. Freitas, J. C. C.; Smith, M. E. *Ann. Rep. NMR Spectrosc.* **2012**, *75*, 25-114.

17. Bräuniger, T.; Jansen, M. Z. *Anorg. Allg. Chem.* **2013**, *639*, 857-879.

18. Chapman, R. P.; Widdifield, C. M.; Bryce, D. L. *Prog. Nucl. Magn. Reson. Spectrosc*. **2009**, *55*, 215-237.

19. Ashbrook, S. E.; Smith, M. E. *Chem. Soc. Rev.* **2006**, *35*, 718-735.

20. Ashbrook, S. E.; Duer, M. J. *Concepts Magn. Reson*. **2006**, *28A*, 183-248.

21. Ashbrook, S. E.; Antonijevic, S.; Berry, A. J.; Wimperis, S. *Chem. Phys. Lett.* **2002**, *364*,

634-642.

22. Amri, M.; Ashbrook, S. E.; Dawson, D. M.; Griffin, J. M.; Walton, R. I.; Wimperis, S. *J. Phys. Chem. C* **2012**, *116*, 15048-15057.

23. Engelhardt, G.; Kentgens, A. P. M.; Koller, H.; Samoson, A. *Solid State Nucl. Magn. Reson*. **1999**, *15*, 171-180.

24. Schurko, R. W. A*cquisition of Wideline Solid-State NMR Spectra of Quadrupolar Nuclei*, eMagRes, 2011. DOI: 10.1002/9780470034590.emrstm1199.

25. O'Dell, L. A; Schurko, R. W. *Chem. Phys. Lett*. **2008**, *464*, 97-102.

26. O'Dell, L. A; Rossini, A. J.; Schurko, R. W. *Chem. Phys. Lett*. **2009**, *468*, 330-335.

27. Schurko, R. W. *Acc. Chem. Res.* **2013**, *46*, 1985-1995.

28. O'Dell, L. A. *Solid State Nucl. Magn. Reson*. **2013**, *55-56*, 28-41.

29. Meiboom S.; Gill, D. *Rev. Sci. Instrum*. **1958**, *29*, 688-691.

30. Madhu, P. K.; Goldbourt, A.; Frydman, L.; Vega, S. *Chem. Phys. Lett*. **1999**, *307*, 41–47.

31. Kentgens, A. P. M.; Verhagen, R. *Chem. Phys. Lett.* **1999**, *300*, 435-443.

32. Seigel, R.; Nakashima, T. K.; Wasylishen, R. E. *Chem. Phys. Lett.* **2004**, *388*, 441-445.

33. Nakashima, T. T.; Wasylishen, R. E. *Sensitivity and Resolution Enhancement of Half-integer Quadrupolar Nuclei in Solid-state NMR*, eMagRes, 2011. DOI: 10.1002/9780470034590.emrstm1200.

34. Perras, F. A.; Viger-Gravel, J.; Burgess, K. M. N.; Bryce, D. L. *Solid State Nucl. Magn. Reson*. **2013**, *51-52*, 1-15.

35. Johnston, K. E.; O'Keefe, C. A.; Gauvin, R. M.; Trébosc, J.; Delevoye, L.; Amoureux, J. P.; Popoff, N.; Taoufik, M.; Oudatchin, K.; Schurko, R. W. *Chem. Eur. J.* **2013**, *19*, 12396-12414.

36. Griffin, J. M.; Berry, A. J.; Ashbrook, S. E. *Solid State Nucl. Magn. Reson*. **2011,** *40*, 91-99.

37. Burgess, K. M. N.; Xu, Y.; Leclerc, M. C.; Bryce, D. L. *Inorg. Chem.* **2014**, *53*, 552−561.

38. Hamaed, H.; Johnston, K. E.; Cooper, B. F. T.; Terskikh, V. V.; Ye, E., Macdonald; C. L. B.; Arnold, D. C.; Schurko, R. W. *Chem. Sci.* **2014**, *5*, 982-995.

39. Hamaed, H.; Ye, E.; Udachin, K.; Schurko, R. W. *J. Phys. Chem. B* **2010**, *114*, 6014–6022.

40. O'Dell, L. A.; Schurko, R. W. *J. Am. Chem. Soc.* **2009**, *131*, 6658-6659.

41. Attrell, R. J.; Widdifield, C. M.; Korobkov, I.; Bryce, D. L. *Cryst. Growth Des.* **2012**, *12*, 1641-1653.

42. Samoson, A.; Lippmaa, E.; Pines, A. *Mol. Phys.* **1988**, *65*, 1013-1018.

43. Mueller, K. T.; Sun, B. Q.; Chingas, G. C.; Zwanziger, J. W.; Terao, T.; Pines, A. *J. Magn. Reson.* **1990**, *86*, 470-487.

44. Frydman, L.; Harwood, J. S. *J. Am. Chem. Soc.* **1995**, *117*, 5367-5368.

45. Goldbourt, A.; Madhu, P. K. *Ann. Rep. NMR Spectrosc.* **2004**, *54*, 81-153.

46. Rocha, J.; Morais, C. M.; Fernandez, C. *Topics in Curr. Chem.* **2005**, *246*, 141-194.

47. Gan, Z. *J. Am. Chem. Soc.* **2000**, *122*, 3242-3243.

48. Ashbrook, S. E.; Wimperis, S. *Prog. Nucl. Magn. Reson. Spectrosc.* **2004**, *45*, 53-108.

49. Gan, Z.; Kwak, H. T. *J. Magn. Reson.* **2004**, *168*, 346-351.

50. Colaux, H.; Dawson, D. M.; Ashbrook, S. E. *J. Phys. Chem. A* DOI: 10.1021/jp505752c.

51. Perras, F. A.; Bryce, D. L. *J. Magn. Reson.* **2011**, *213*, 82-89.

52. Perras, F. A.; Bryce, D. L. *J. Chem. Phys.* **2013**, *138*, 174202.

53. Perras, F. A.; Bryce, D. L. *J. Magn. Reson.* **2014**, *242*, 23-32.

54. Ashbrook, S. E.; McManus, J.; Thrippleton, M. J.; Wimperis, S. *Prog. Nucl. Magn. Reson. Spectrosc.* **2009**, *55*, 160-181.

55. Sternheimer, R. *Phys. Rev.* **1954**, *95*, 736-750.

56. O'Dell, L. *Prog. Nucl. Magn. Reson. Spectrosc.* **2011**, *59*, 295-318.

57. Hoatson, G. L; Vold, R. L. *^{2}H NMR Spectroscopy of Solids and Liquid Crystals*, NMR Basic Principles Prog., **1994**, *32*, 1-67.

58. Colin, J. F.; Bataille, T.; Ashbrook, S. E.; Audebrand, N.; Le Polles, L.; Pivan, J. Y.; Le Fur, E. *Inorg. Chem.* **2006**, *45*, 6034-6040.

59. Johnston, K. E.; Tang, C. C.; Parker, J. E.; Knight, K. S.; Lightfoot, P.; Ashbrook, S. E. *J. Am. Chem. Soc.* **2010**, *132*, 8732-8746.

60. Hanna, J. V.; Smith, M. E.; Whitfield, H. J. *J. Am. Chem. Soc.* **1996**, *118*, 5772-5777.

61. Sheppard, D.; Tugarinov, V. *J. Magn. Reson.* **2010**, *203*, 316-322.

62. Alemany, L. B.; Steuernagel, S.; Amoureux, J. P.; Callender, R. L.; Barron, A. R. *Solid State Nucl. Magn. Reson.* **1999**, *14*, 1-18.

63. Pickard, C. J.; Mauri, F. *Phys. Rev. B*, **2001**, *63*, 245101.

64. Cuny, J.; Messaoudi, S.; Alonzo, V.; Furet, E.; Halet, J. F.; Le Fur, E.; Ashbrook, S. E.; Pickard, C. J.; Gautier, R.; Le Polles, L. *J. Comp. Chem.* **2008**, *29*, 2279-2287.

65. Charpentier, T. *Solid State Nucl. Magn. Reson.* **2011**, *40*, 1-20.

66. Bonhomme, C.; Gervais, C.; Babonneau, F.; Coelho, C.; Pourpoint, F.; Azaïs, T.; Ashbrook, S. E.; Griffin, J. M.; Yates, J. R.; Mauri, F.; Pickard, C. J. *Chem. Rev.* **2012**, *112*, 5733-5779.

67. Ashbrook, S. E.; Le Polles, L.; Pickard, C. J.; Berry, A. J.; Wimperis, S.; Farnan, I. *Phys. Chem. Chem. Phys.* **2007**, *9,* 1587-1598.

68. Ashbrook, S. E.; Berry, A. J.; Hibberson, W. O.; Steuernagel, S.; Wimperis, S. *J. Am. Chem. Soc.* **2003**, *125*, 11824-11825.

69. Harris, R. K.; Wasylishen, R. E.; Duer, M. J. (Eds), *NMR Crystallography*, John Wiley & Sons Ltd, Chichester, 2009.

70. Martineau, C.; Cadiau, A.; Bouchevreau, B.; Senker, J.; Taulelle, F.; Adil, K. *Dalton Trans.* **2012**, *41*, 6232-6241.

71. Amoureux, J. P.; Trebosc, J.; Delevoye, L.; Lafon, O.; Hu, B.; Wang, Q. *Solid State Nucl. Magn. Reson.* **2009**, *35*, 12-18.

72. Ashbrook, S. E.; Cutajar, M.; Pickard, C. J.; Walton, R. I.; Wimperis, S. *Phys. Chem. Chem. Phys.* **2008**, *10*, 5754-5764.

73. Wiench, J. W.; Pruski, M. *Solid State Nucl. Magn. Reson.* **2004**, *26*, 51-55.

74. Montouillout, V.; Morais, C. M.; Douy, A.; Fayon, F.; Massiot, D. *Magn. Reson. Chem.* **2006**, *44*, 770-775.

75. Iuga, D.; Morais, C.; Gan, Z.; Neuville, D. R.; Cormier, L.; Massiot, D. *J. Am. Chem. Soc.,* **2005**, *127*, 11540‑11541.

76. Ashbrook, S. E.; Wimperis, S. *Mol. Phys.* **2000**, *98*, 1-26.

77. Amoureux, J. P.; Pruski, M. *Mol. Phys.* **2002**, *100*, 1595-1613.

78. Ashbrook, S. E.; Wimperis, S. *J. Chem. Phys.* **2004**, *120*, 2719-2731.

79. Ashbrook, S. E.; Wimperis, S. *J. Chem. Phys.* **2009**, *131*, 194509.

80. Lu, X.; Lafon, O.; Trebosc, J.; Tricot, G.; Delevoye, L.; Mear, F.; Montagne, L.;

Amoureux, J. P. *J. Chem. Phys.* **2012**, *137*, 144201.

81. Hu, B.; Trebosc, J.; Amoureux, J. P. *J. Magn. Reson.* **2008,** *192,* 112-122.

82. Levitt, M. H. *J. Chem. Phys.* **2008**, *128*, 52205.

83. Mali, G.; Fink, G.; Taulelle, F. *J. Chem. Phys.* **2004**, *120*, 2835-2845.

84. Eden, M.; Zhou, D.; Yu, J. *Chem. Phys. Lett.* **2006**, 431, 397-403.

85. Gan, Z. *J. Am. Chem. Soc.* **2006**, *128*, 6040-6041.

86. Cavadini, S.; Antonijevic, A.; Lupulescu, A.; Bodenhausen, G. *J. Magn. Reson.* **2006**, *182*, 168-172.

87. Cavadini, S. *Prog. Nucl. Magn. Reson. Spectrosc.* **2010**, *56*, 46-77.

88. de Lacaillerie, J. B. D.; Fretigny, C.; Massiot, D. *J. Magn. Reson.* **2008**, *192*, 244-251.

89. Ferrara, C.; Tealdi, C.; Pedone, A.; Menziani, M. C.; Rossini, A. J.; Pintacuda, G.; Mustarelli, P. *J. Phys. Chem. C* **2013**, *117*, 23451-23458.

90. Johnston, K. E.; Mitchell, M. R.; Blanc, F.; Lightfoot, P.; Ashbrook, S. E. *J. Phys. Chem. C* **2013**, *117*, 2252-2265.

91. Florian, P.; Veron, E.; Green, T. F. G.; Yates, J. R.; Massiot, D. *Chem. Mater.* **2012**, *24*, 4068-4079.

92. Seymour, V. R.; Eschenroeder, E. C. V.; Castro, M.; Wright, P. A.; Ashbrook, S. E. *CrystEngComm* **2013**, *15*, 8668-8679.

93. Blanc, F.; Middlemiss, D. S.; Gan, Z.; Grey, C. P. *J. Am. Chem. Soc.* **2011**, *133*, 17662-17672.

94. Ashbrook, S. E.; Dawson, D. M. *Acc. Chem. Res.* **2013**, *46*, 1964-1974.

95. Florian, P.; Massiot, D. *CrystEngComm* **2013**, *15*, 8623-8626.

96. O'Dell, L. A.; Ratcliffe, C. I. *Quadrupolar NMR to Investigate Dynamics in Solid Materials*, eMagRes, 2011. DOI: 10.1002/9780470034590.emrstm1209.

97. Vold, R. L.; Hoatson, G. L. *J. Magn. Reson.* **2009**, *198*, 57-72.

98. Cutajar, M.; Ashbrook, S. E.; Wimperis, S. *Chem. Phys. Lett.* **2006**. *423*, 276-281.

99. Thrippleton, M. J.; Cutajar, M.; Wimperis, S. *Chem. Phys. Lett.* **2008**, *452*, 233-238.

100. Hampson, M. R.; Hodgkinson, P.; Evans, J. S. O.; Harris, R. K.; King, I. J.; Allen, S.; Fayon, F. *Chem. Commun.* **2004**, *4*, 392-393.

101. Antonijevic, S.; Ashbrook, S. E.; Biedasek, S.; Walton, R. I.; Wimperis, S.; Yang, H. *J. Am. Chem. Soc.* **2006**, *128*, 8054-8062.

102. Ashbrook, S. E.; Berry, A. J.; Wimperis, S. *J. Am. Chem. Soc.* **2001**, *123*, 6360-6366.

103. Griffin, J. M.; Wimperis, S.; Berry, A. J.; Pickard, C. J.; Ashbrook, S. E. *J. Phys. Chem. C* **2008**, *113*, 465-471.

104. Griffin, J. M.; Miller, A. J.; Berry, A. J.; Wimperis, S.; Ashbrook, S. E. *Phys. Chem. Chem. Phys.* **2010**, *12*, 2989-2998.

105. Griffin, J. M.; Yates, J. R.; Berry, A. J.; Wimperis, S.; Ashbrook, S. E. *J. Am. Chem. Soc.* **2010**, *132*, 15651-15660.

106. Ashbrook, S. E.; Cutajar, M.; Griffin, J. M.; Lethbridge, Z. A.; Walton, R. I.; Wimperis, S. *J. Phys. Chem. C.* **2009**, *113*, 10780-10789.

107. Blanc, F.; Leskes, M.; Grey, C. P. *Acc. Chem. Res.* **2013**, *46*, 1952-1963.

108. Grey, C. P.; Dupre, N. *Chem. Rev.* **2004**, *104*, 4493-4512.

109. Blanc, F.; Spencer, L.; Goward, G. R. *Quadrupolar NMR of Ionic Conductors, Batteries, and Other Energy-related Materials*, 2011. DOI: 10.1002/9780470034590.emrstm1215.

110. Yoon, W. S.; Grey, C. P.; Balasubramanian, M.; Yang, X. Q.; Fischer, D. A.; McBreen, J. *Electrochem. Solid State Lett.* **2004**, *7*, A53-A55.

111. Letellier, M.; Chevallier, F.; Clinard, C.; Frackowiak, E.; Rouzaud, J. N.; Beguin, F.; Morcrette, M.; Tarascon, J. M. *J. Chem. Phys.* **2003**, *118*, 6038-6045.

112. Key, B.; Bhattacharyya, R.; Morcrette, M.; Seznec, V.; Tarascon, J. M.; Grey, C. P. *J. Am. Chem. Soc.* **2009**, *131*, 9239-9249.

113. Wang, H.; Köster, T. K. J.; Trease, N. M.; Ségalini, J.; Taberna, P. L.; Simon, P.; Gogotsi, Y.; Grey, C. P. *J. Am. Chem. Soc.* **2011**, *133*, 19270-19273.

114. Kim, N.; Stebbins, J. F. *Chem. Mater.* **2007**, *19*, 5742-5747.

115. Wright, P. A. *Microporous Framework Solids*, The Royal Society of Chemistry, 1st edn, 2008.

116. Ashbrook, S. E.; Dawson, D. M.; Seymour, V. R. *Phys. Chem. Chem. Phys.* **2014**, *16*, 8223-8242.

117. Taulelle, F.; Bouchevreau, B.; Martineau, C. *CrystEngComm* **2013**, *15*, 8613-8622.

118. Martineau, C.; Bouchevreau, B.; Tian, Z.; Lohmeier, S. J.; Behrens, P.; Taulelle, F. *Chem. Mater*. **2011**, *23*, 4799-4809.

119. Martineau, C.; Mellot-Draznieks, C.; Taulelle, F. *Phys. Chem. Chem. Phys*. **2011**, *13*, 18078-18087.

120. Beitone, L.; Huguenard, C.; Gansmüller, A.; Henry, M.; Taulelle, F.; Loiseau, T.; Férey, G. *J. Am. Chem. Soc*. **2003**, *125*, 9120-9110.

121. Morais, C. M.; Montouillout, V.; Deschamps, M.; Iuga, D.; Fayon, F.; Paz, F. A. A.; Rocha, J.; Fernandez, C.; Massiot, D. *Magn. Reson. Chem*. **2009**, *47*, 942-947.

122. Bull, L. M.; Bussemer, B.; Anupold, T.; Reinhold, A.; Samoson, A.; Sauer, J.; Cheetham, A. K.; Dupree, R. *J. Am. Chem. Soc*. **2000**, *122*, 4948-4958.

123. Griffin, J. M.; Clark, L.; Seymour, V. R.; Aldous, D. W.; Dawson, D. M.; Iuga, D.; Morris, R. E.; Ashbrook, S. E. *Chem. Sci*. **2012**, *3*, 2293-2300.

124. He, P.; Xu, J.; Terskikh, V. V.; Sutrisno, A.; Nie, H. Y.; Huang, Y. *J. Phys. Chem. C* **2013**, *117*, 16953-16960.

125. Loiseau, T.; Serre, C.; Huguenard, C.; Fink, G.; Taulelle, F.; Henry, M.; Bataille, T.; Férey, G. *Chem. Eur. J*. **2004**, *10*, 1373-1382.

126. Mowat, J. P.; Seymour, V. R.; Griffin, J. M.; Thompson, S. P.; Slawin, A. M.; Fairen-Jimenez, D.; Duren, T.; Ashbrook, S. E.; Wright, P. A. *Dalton Trans*. **2012**, *41*, 3937-3941.

127. Mowat, J. P. S.; Miller, S. R.; Griffin, J. M.; Seymour, V. R.; Ashbrook, S. E.; Thompson, S. P.; Fairen-Jimenez, Banu, D. A. M.; Duren T.; Wright, P. A. *Inorg. Chem.* **2011**, *50*, 10844.

128. Kolokolov, D. I.; Jobic, H.; Stepanov, A. G.; Guillerm, V.; Devic, T.; Serre C.; Férey, G. *Angew. Chem. Int. Ed.* **2010**, *49*, 4791-4794.

129. Loewenstein, W. *Am. Mineral*. **1953**, *39*, 92-96.

130. Stebbins, J. F.; Farnan, I.; Williams E. H.; Roux, J. *Phys. Chem. Mineral.* **1989**, *16*, 763-766.

131. Stebbins, J. F. *Am. Mineral*. **1997**, *81*, 1315-1320.

132. Frost, D. J.; Poe, B. T.; Tronnes, R. G.; Liebske, C.; Duba, A.; Rubie, D. C. *Phys. Earth Planet. Int.* **2004**, *143-144*, 507-514.

133. Griffin, J. M.; Berry, A. J.; Frost, D. J.; Wimperis, S.; Ashbrook, S. E. *Chem. Sci*. **2013**, *4*, 1523-1538.

134. Eckert, H. *Amorphous Materials*, 2007, DOI: 10.1002/9780470034590.emrstm0009.

135. Florian, P.; Vermillion, K. E.; Grandinetti, P. J.; Farnan, I.; Stebbins, J. F. *J. Am. Chem. Soc.* **1996**, *118*, 3493-3497.

136. Farnan, I.; Grandinetti, P. J.; Baltisberger, J. H.; Stebbins, J. F.; Werner, U.; Eastman, M. A.; Pines, A. *Nature* **1992**, *358*, 31-35.

137. Dubinsky, E. V.; Stebbins, J. F. *Am. Mineral*. **2006**, *91*, 753-761.

138. Wu, G. *Biochem. Cell Biol*. **1998**, *76*, 429-442.

139. Polenova, T.; Lipton, A. S.; Ellis, P. D. *Quadrupolar NMR of Metal Nuclides in Biological Materials*, 2011. DOI: 10.1002/9780470034590.emrstm1222.

140. Lipton, A. S.; Heck, R. W.; Hernick, M.; Fierke, C. A.; Ellis, P. D. *J. Am. Chem. Soc.* **2008**, *130*, 12671-12679.

141. Laurencin, D.; Smith, M. E. *Prog. Nucl. Magn. Reson. Spectrosc*. **2013**, *68*, 1-40.

142. Laurencin, D.; Wong, A.; Chrzanowski, W.; Knowles, J. C.; Qiu, D.; Pickup, D. M.; Newport, R. J; Gan Z.; Duer, M. J; Smith, M. E. *Phys. Chem. Chem. Phys*. **2010**, *12*, 1081-1091.

143. Pound, R. V. *Phys. Rev*. **1950**, *79*, 685-702.

144. Frydman, L.; Scherf, T.; Lupulescu, A. *Proc. Natl. Acad. Sci*. **2002**, *99*, 15858-15862.

145. Takeda, K. *Solid State Nucl. Magn. Reson*. **2012**, *47-48*, 1-9.

146. Wind, R. A. *Dynamic Nuclear Polarization and High-Resolution NMR of Solids*, eMagRes, 2007, DOI: 10.1002/9780470034590.emrstm0140.

147. Blanc, F.; Sperrin, L.; Jefferson, D. A.; Pawsey, S.; Rosay, M.; Grey, C. P. *J. Am. Chem. Soc.* **2013**, *135*, 2975-2978.

148. Lee, D.; Takahashi, H.; Thankamony, A. S. L.; Dacquin, J. P.; Bardet, M.; Lafon, O.; Paëpe, G. *J. Am. Chem. Soc.* **2012**, *134*, 18491-18494.

149. Vitzthum, V.; Miéville, P.; Carnevale, D.; Caporini, M. A.; Gajan, D.; Copéret, C.; Lelli, M.; Zagdoun, A.; Rossini, A. J.; Lesage, A.; Emsley, L.; Bodenhausen G. *Chem. Commun*. **2012**, *48*, 1988-1990.

150. Pickard, C. J.; Needs, R. J. *J. Phys.*: *Condens. Mat*. **2011**, *23*, 053201.

151. Zheng, A.; Huang, S. J.; Wang, Q.; Zhang, H.; Deng F.; Liu, S. B. *Chin. J. Catal.* **2013**, *34*, 436-491.

152. Roberts, S. T.; Renshaw, M. P.; Lutecki, M.; McGregor, J.; Sederman, A. J.; Mantle, M. D.; Gladden, L. F. *Chem. Commun.* **2013**, *49*, 10519-10521.

Table 1. Properties of selected quadrupolar nuclei.

Nucleus	I	N (%)	γ / 10^7 rad s^{-1} T^{-1}	ν_0 / MHz[a]	Receptivity[b]	Q / fm^2
^{2}H	1	0.01	4.107	92.12	1.11×10^{-6}	0.286
^{6}Li	1	7.59	3.937	88.32	6.45×10^{-4}	−0.0808
^{7}Li	3/2	92.41	10.398	233.23	2.71×10^{-1}	−4.01
^{10}B	3	19.9	2.875	64.48	3.95×10^{-3}	8.459
^{11}B	3/2	80.1	8.585	192.55	1.32×10^{-1}	4.059
^{14}N	1	99.64	1.934	43.38	1.00×10^{-3}	2.044
^{17}O	5/2	0.04	−3.628	81.36	1.10×10^{-5}	–2.558
^{23}Na	3/2	100.00	7.081	158.75	9.26×10^{-2}	10.4
^{25}Mg	5/2	10.00	−1.639	36.74	2.68×10^{-4}	19.94
^{27}Al	5/2	100.00	6.976	156.38	2.06×10^{-1}	14.66
^{33}S	3/2	0.75	2.056	46.07	1.70×10^{-5}	–6.78
^{35}Cl	3/2	75.76	2.624	58.80	3.56×10^{-3}	–8.165
^{37}Cl	3/2	24.24	2.184	48.95	6.58×10^{-4}	–6.435
^{39}K	3/2	93.26	1.250	28.00	4.74×10^{-4}	5.85
^{43}Ca	7/2	0.14	–1.80	40.39	8.64×10^{-6}	–4.08
^{45}Sc	7/2	100.00	6.51	145.78	3.01×10^{-1}	–22.0
^{47}Ti	5/2	7.44	–1.51	33.83	1.56×10^{-4}	30.2
^{49}Ti	7/2	5.41	–1.51	33.84	2.04×10^{-4}	24.7
^{51}V	7/2	99.75	7.05	157.85	3.81×10^{-1}	–5.2
^{55}Mn	5/2	100.00	6.65	148.77	1.78×10^{-1}	33
^{59}Co	7/2	100.00	6.33	142.39	2.81×10^{-1}	42
^{67}Zn	5/2	4.10	1.68	37.55	1.17×10^{-4}	15.0
^{69}Ga	3/2	60.11	6.44	144.04	4.16×10^{-2}	17.1
^{71}Ga	3/2	39.89	8.18	183.02	5.66×10^{-2}	10.7
^{79}Br	3/2	50.69	6.73	150.37	4.00×10^{-2}	30.5

^{81}Br	3/2	49.31	7.25	162.07	4.86×10^{-2}	25.4
^{87}Rb	3/2	27.83	8.79	196.37	4.88×10^{-2}	13.35
^{91}Zr	5/2	11.22	–2.50	55.79	1.05×10^{-3}	–17.6
^{93}Nb	9/2	100.00	6.57	146.89	4.84×10^{-1}	–32
^{133}Cs	7/2	100.00	3.53	78.71	4.74×10^{-2}	–0.343
^{139}La	7/2	99.91	3.81	84.77	5.91×10^{-2}	20

[a] Larmor frequency at 14.1 T

[b] Receptivity quoted relative to ^{1}H

Figure Captions

Figure 1. Schematic energy level diagrams, showing the effect of the Zeeman and first-order quadrupolar interactions for nuclei with (a) I = 1 and (b) I = 3/2. For I = 3/2, the central transition (CT) is unaffected by the first-order quadrupolar interaction whereas the satellite transitions (ST) show a significant perturbation. (All transitions will be affected by the second-order quadrupolar interaction). Also shown are simulations of the resulting single-crystal NMR spectra (now showing 2I non degenerate transitions) and corresponding powder lineshapes.

Figure 2. (a) Schematic depiction of the MAS experiment, where a polycrystalline sample is rotated about an axis inclined at an angle of 54.736° to the external magnetic field, B_0. (b) Rotors of varying outer diameter and the maximum MAS rates that can be achieved. (c) Effect of MAS (14 kHz) on the ^{2}H (9.4 T) first-order quadrupolar-broadened lineshape of oxalic acid dihydrate ($D_2C_2O_4.2D_2O$). The lineshape consists of a manifold of spinning sidebands, in each of which resonances from the two distinct ^{2}H sites are resolved. (d) Effect of MAS (14 kHz) on the ^{71}Ga (14.1 T) second-order quadrupolar-broadened CT lineshape of $GaPO_4$ berlinite. Under MAS, a powder-pattern lineshape is observed (although narrowed in comparison to the static case), shifted from δ_{iso} (shown by the dashed line) by the isotropic quadrupolar shift.

Figure 3. ^{23}Na (14 kHz, 14.1 T) (a) MAS and (b) triple-quantum MAS spectra of $Na_4P_2O_7$. (c) Cross sections, extracted parallel to δ_2, for each of the four Na species, and corresponding fits with the relevant NMR parameters given. (d) ^{11}B DOR (top, experiment and two simulations) and MAS (bottom, experiment and simulation) spectra of manganese catecholboryl pentacarbonyl. Reprinted with permission from Ref. 52. Copyright 2014, AIP Publishing LLC.

Figure 4. Three-dimensional plot showing the receptivity ($\log_{10}$ γ^3N (I (I + 1)), quoted relative to ^{1}H), gyromagnetic ratio (γ, quoted relative to ^{1}H) and quadrupole moment ($\log_{10}$ |Q|) for quadrupolar nuclides. Commonly-studied nuclei (*i.e.*, those given in Table 1) are marked.

Figure 5. (a) ^{23}Na (12.5 kHz, 9.4 T) MAS NMR spectrum of $Na_2[(VO)_2(HPO_4)_2C_2O_4]$,$2H_2O$, and corresponding simulated fit, showing two overlapping resonances, confirming the space group as $P2_1$ not $P2_1/m$. Adapted with permission from Ref. 58. Copyright 2006 American Chemical Society. (b) ^{71}Ga (25-30 kHz, 20.0 T) MAS NMR spectrum of as-made and calcined GaPO-34, showing the change in the coordination number of the framework species upon calcination. Adapted with permission from Ref. 22. Copyright 2012 American Chemical Society. (c) Structure of wadsleyite, β-Mg_2SiO_4, cross sections (extracted from STMAS spectra) and lineshapes generated using parameters calculated by DFT for each of the four O species. Adapted from Ref. 67 with permission from the PCCP Owner Societies.

Figure 6. NMR spectra of as-made STA-2. MAS NMR spectra and plots of chemical shifts arising from DFT calculations for possible structural models with differing positions of the charge-balancing hydroxyls for (a) ^{31}P (14 kHz, 14.1 T) and (b) ^{27}Al (14 kHz, 14.1 T). (c) Two-dimensional ^{27}Al/^{31}P (12.5 kHz, 20.0 T) HETCOR spectrum and (overlaid) cross-peak position from DFT calculations. (d) Schematic of framework-bound hydroxyl anion in a cancrinite cage. Good agreement with experiment is only obtained for models where hydroxyls are in different cancrinite cages and do not share a double four membered ring. Adapted from Ref. 92, published by the Royal Society of Chemistry.

Figure 7. (a) The two possible proton positions, H1 and H2, that are associated with each hydroxyl group in clinohumite, $4Mg_2SiO_4.Mg(OH)_2$, and models used in the DFT calculations. ^{17}O (8 kHz, 9.4 T) (b) MQMAS and (c) STMAS spectra of clinohumite. Also shown in (b, c), are spectra resulting from the summation and averaging of simulated ^{17}O

isotropic spectra calculated for different arrangements of the hydroxyl groups. In (c), STMAS spectra are simulated using the calculated NMR parameters for the different structural models, and an additional line broadening determined using a simple model for motional broadening. (d) variable temperature ^{2}H (10 kHz, 9.4 T) MAS NMR spectra of deuterated clinohumite and (e) resulting Arrhenius plot to extract the activation energy. Adapted with permission from Ref. 103. Copyright 2009 American Chemical Society. Adapted from Ref. 104 with permission from the PCCP Owner Societies.

Figure 8. (a) Schematic diagram of a modified supercapacitor cell used for *in situ* NMR analysis. (b) Stacked plot of ^{11}B NMR spectra obtained whilst charging the modified supercapacitor between +2 V and −2 V. (c) Integrated ^{11}B intensity from (b) plotted as a function of voltage, showing the loss of strongly-bound BF_4^- species as the voltage becomes more negative. Adapted with permission from Ref. 113. Copyright 2011 American Chemical Society.

Figure 9. (a) ^{19}F-^{27}Al (11.7 T, 15 kHz) J-HMQC spectrum of AlPO-CJ2, enabling the determination of the OH^-/F^- distribution in this framework material. Adapted from Ref. 119 with permission of the PCCP Owner Societies. (b) ^{31}P (9.4/17.6 T, 14 kHz) and ^{27}Al (17.6 T, 14 kHz) MAS and MQMAS spectra of AlPO-40. Adapted from Ref. 121 with permission from Wiley.

Figure 10. (a, b) ^{17}O (20.0 T, 30 kHz) STMAS NMR spectra of (a) anhydrous and (b) hydrous (3% by weight) wadsleyite, β-Mg_2SiO_4, showing a decrease in the intensity of the resonance attributed to O1 and a corresponding increase in a broader resonance thought to be associated with hydroxyl oxygens. (c) $^{1}H/^{17}O$ (20.0 T, 30 kHz) CP HETCOR spectrum of hydrous wadsleyite, showing two different types of hydroxyl species. (d) Possible structural models for the defect sites in hydrous wadsleyite determined using DFT calculations. Adapted from Ref. 133, published by the Royal Society of Chemistry.

Figure 11. (a) Changes in the structure of the zinc-containing protein *Aquifex aeolicus* LpxC with pH variation, showing deprotonation initially of a glutamine, and subsequently a histdine, residue. (b) ^{67}Zn (18.8 T) CPMG spectra of a static sample of wild type LpxC at (b) pH 8.7 and (c) pH 6. Simulated lineshapes, shown in red highlight the change in C_Q observed. Adapted with permission from Ref. 140. Copyright 2008 American Chemical Society.

Figure 1

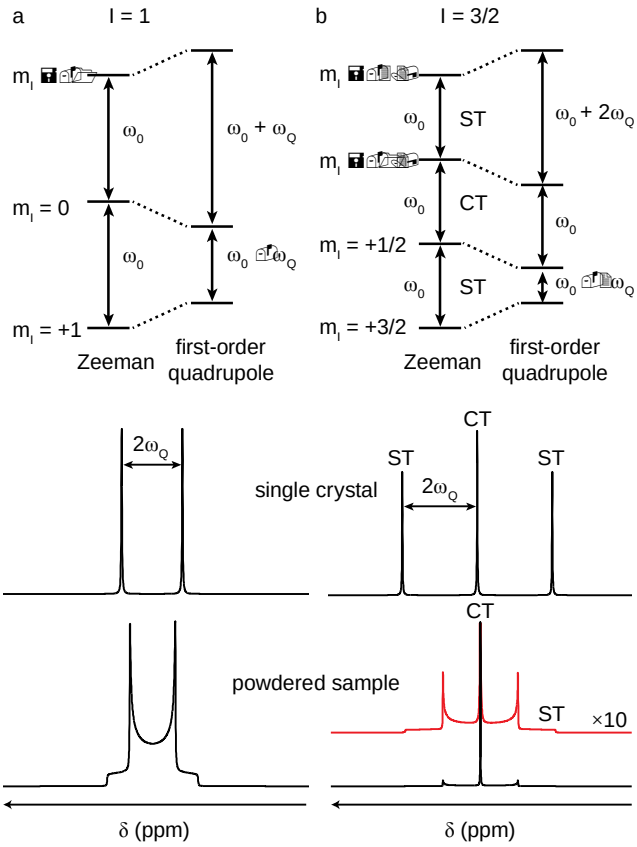

Figure 2

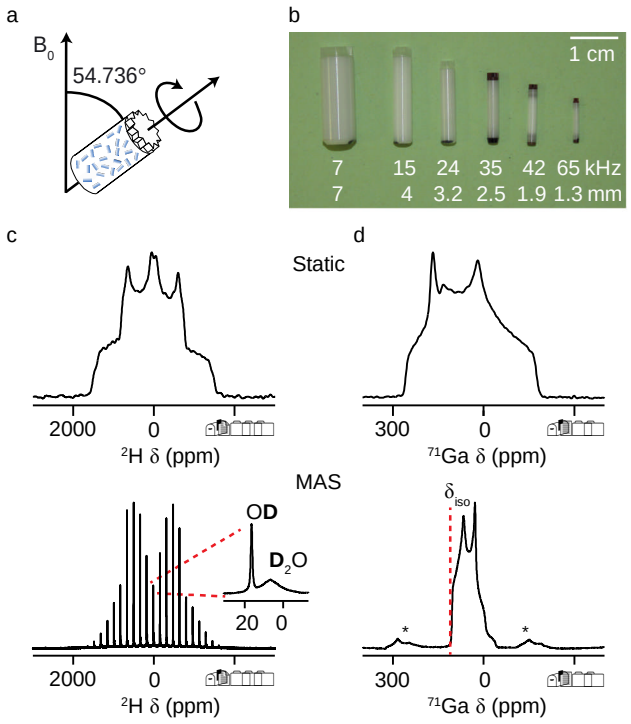

Figure 3

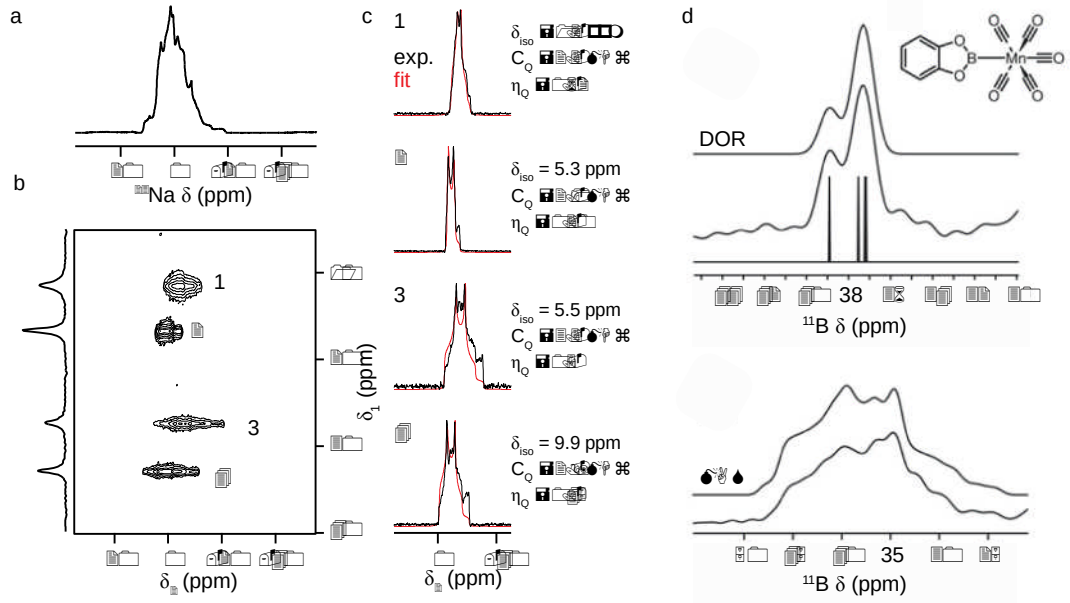

Figure 4

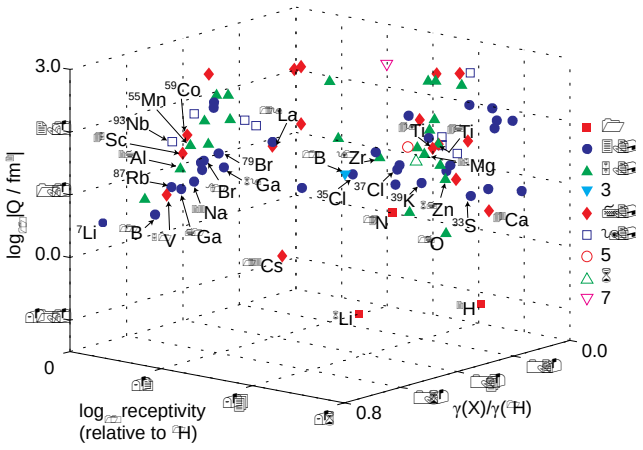

Figure 5

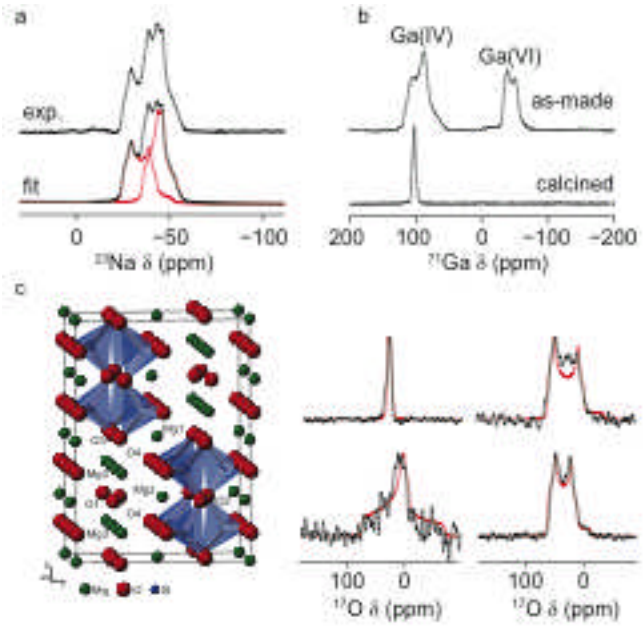

Figure 6

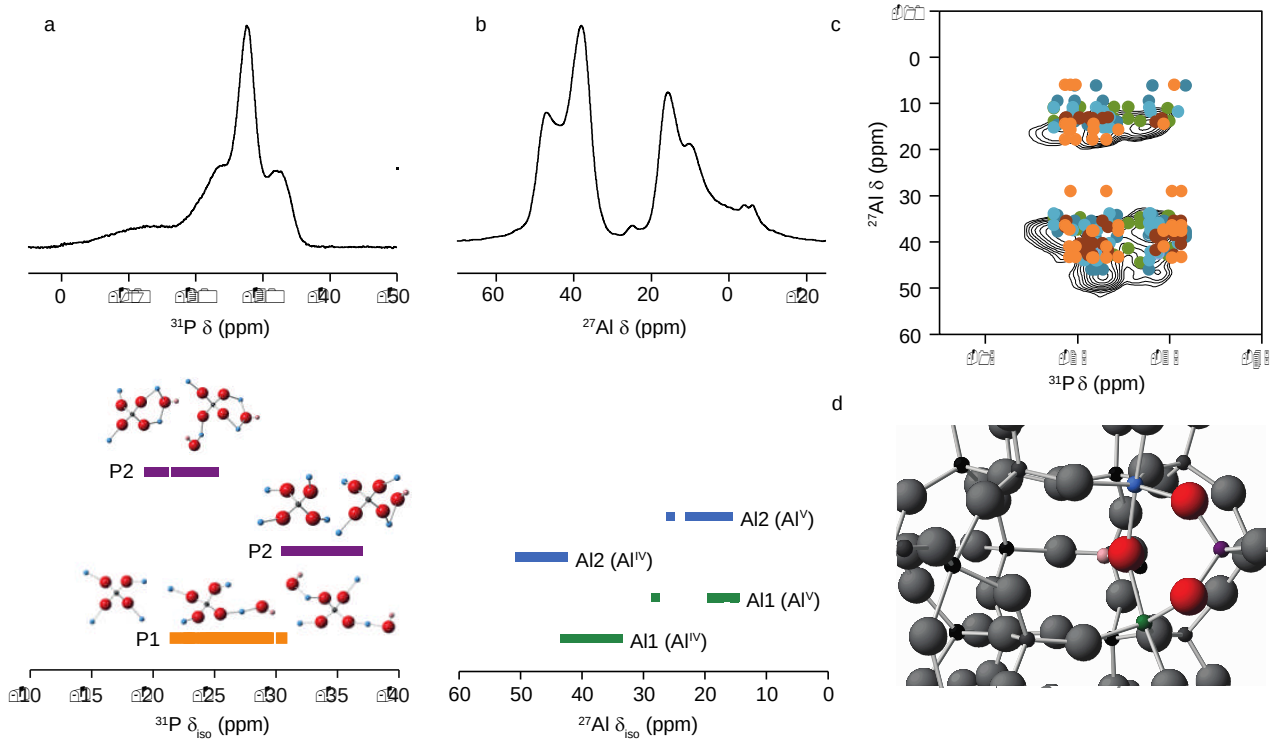

Figure 7

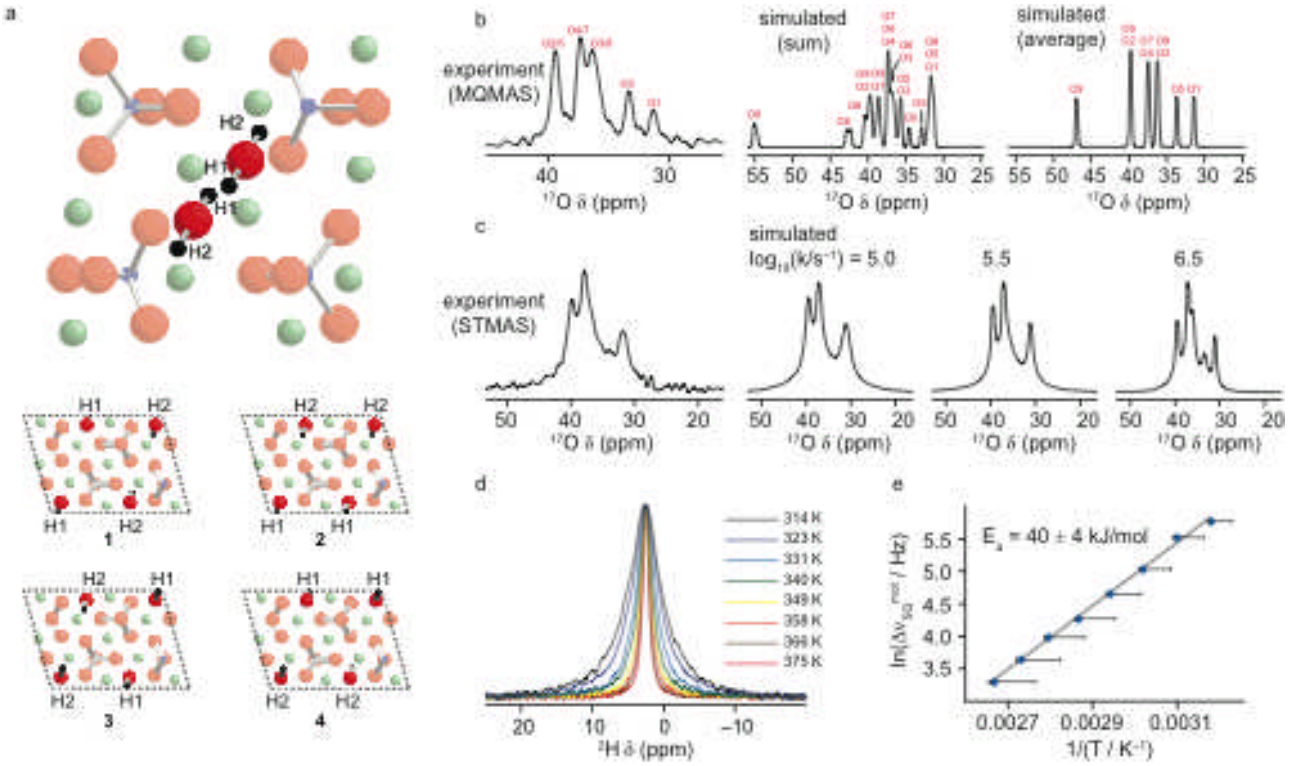
a
H2
H1
H1
H2
H1
H2
H2
H2
1
H1
H1
2
H2
H1
H2
H1
3
H1
H1
H2
H2
4
b
experiment
(MQMAS)
40
30
^{17}O δ (ppm)
simulated
(sum)
55 50 45 40 35 30 25
^{17}O δ (ppm)
simulated
(average)
55 50 45 40 35 30 25
^{17}O δ (ppm)
c
experiment
(STMAS)
50 40 30 20
^{17}O δ (ppm)
simulated
log$_{10}$(k/s^{-1}) = 5.0
5.5
6.5
50 40 30 20
^{17}O δ (ppm)
d
314 K
323 K
331 K
340 K
349 K
358 K
368 K
375 K
20 10 0 −10
^{2}H δ (ppm)
e
E$_a$ = 40 ± 4 kJ/mol
ln(Δν$_{1/2}^{mod}$ / Hz)
5.5
5.0
4.5
4.0
3.5
0.0027 0.0029 0.0031
1/(T / K^{-1})

Figure 8

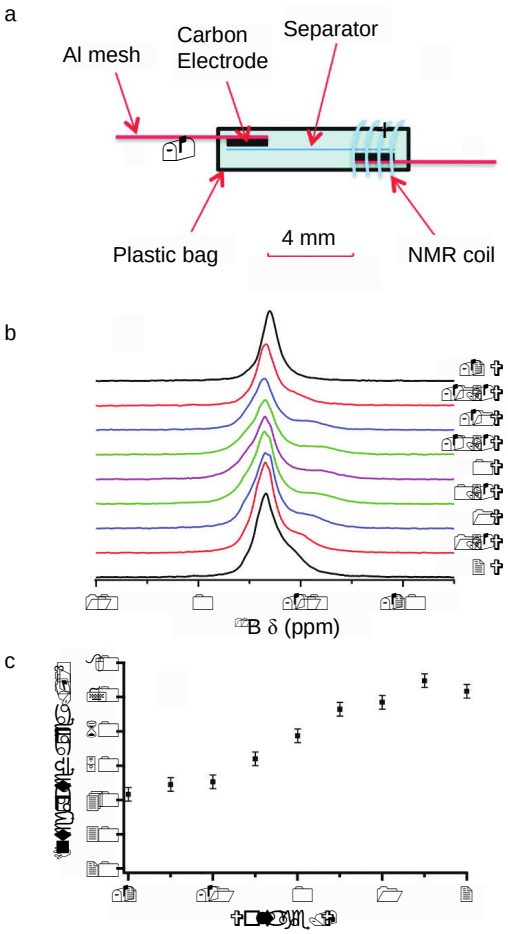
a
Al mesh
Carbon
Electrode
Separator
Plastic bag
4 mm
NMR coil
b
B δ (ppm)
c

Figure 9

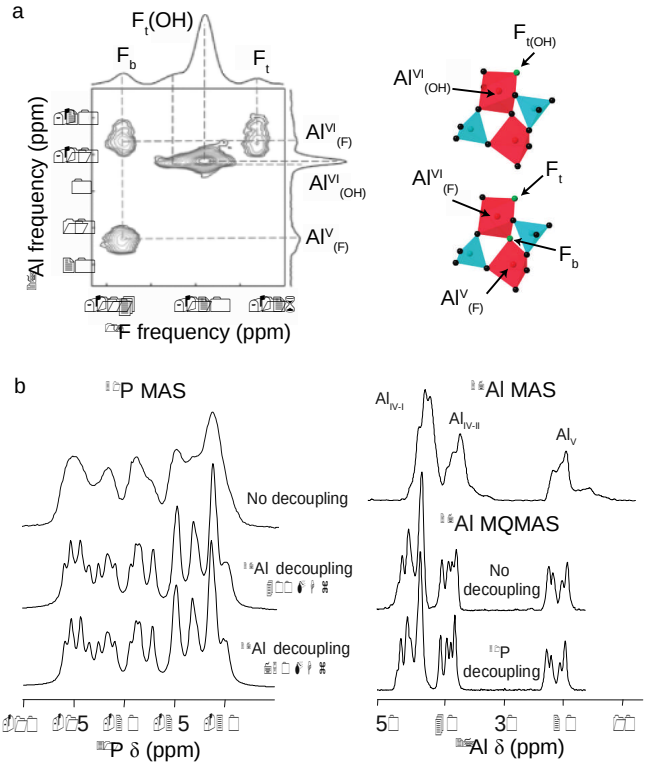

Figure 10

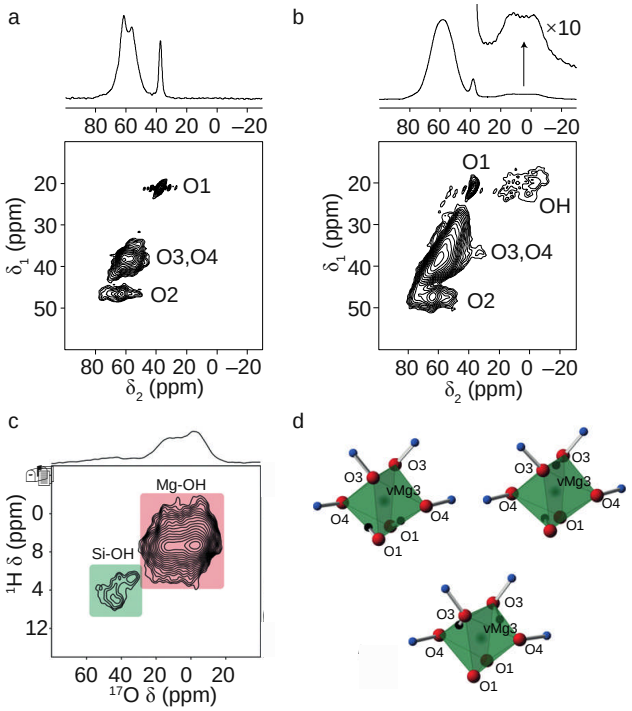

Figure 11

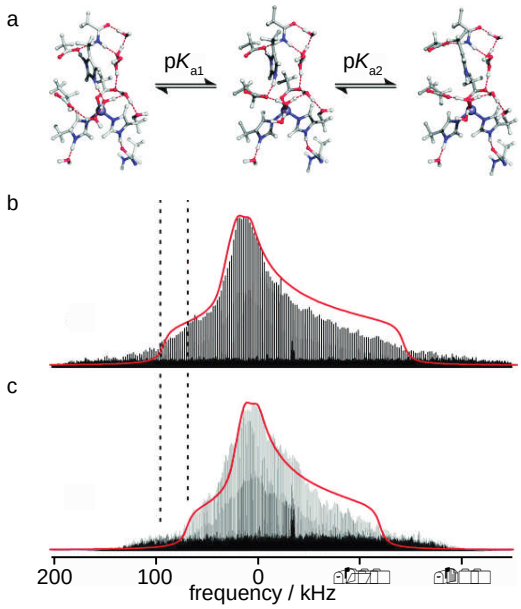

TOC Graphic